Size Reduction of Square Microstrip Patch Antenna by Using Metamaterials Structure

Moataz Moftah Hamad Yousiff

Submitted to the
Institute of Graduate Studies and Research
in partial fulfilment of the requirements for the degree of

Master of Science
in
Electrical and Electronic Engineering

Eastern Mediterranean University
July 2018
Gazimağusa, North Cyprus

Approval of the Institute of Graduate Studies and Research

_____

Assoc. Prof. Dr. Ali Hakan Ulusoy
Acting Director

I certify that this thesis satisfies all the requirements as a thesis for the degree of Master of Science in Electrical and Electronic Engineering.

_____

Prof. Dr. Hasan Demirel
Chair, Department of Electrical and Electronic Engineering

We certify that we have read this thesis and that in our opinion it is fully adequate in scope and quality as a thesis for the degree of Master of Science in Electrical and Electronic Engineering.

_____

Asst. Prof. Dr. Rasime Uyguroğlu
Supervisor

Examining Committee

1. Prof. Dr. Hasan Demirel _____

2. Assoc. Prof. Dr. Mehmet Kuşaf _____

3. Asst. Prof. Dr. Rasime Uyguroğlu _____

ABSTRACT

The focus of this study is to investigate size reduction of Conventional Microstrip Patch Antenna (CMPA), using metamaterial structure. Metamaterial is a Complementary Split Ring Resonator (CSRR) unit cell which has negative permittivity ($\varepsilon < 0$) and positive permeability ($\mu > 0$). The CSRR response is verified in simulation based on scattering parameters by using Nicolson-Ross-Weir (NRW) method. Results show that the relative permittivity is negative at the resonant frequency of CSRR.

This study also presents the design and simulation of the CMPA and Miniaturized Microstrip Patch Antennas (MMPA) at 5.15 GHz resonant frequency. The reduction ratio reaches to 80.7 % by applying metamaterial structure via CSRR in the substrate. Those antennas were simulated using Computer Simulation Technology Microwave Studio (CST MWS).

Keywords: Metamaterials, CSRR Unit Cell, Conventional Microstrip Patch Antenna, Miniaturized Microstrip Patch Antenna.

ÖZ

Bu çalışmanın amacı, meta malzeme yapıları kullanarak, Geleneksel Mikroşerit Yama Anteninin boyut küçültmesini araştırmaktır. Meta malzeme yapı, negatif permitivite ($\varepsilon < 0$) ve pozitif pemeabilite ($\mu > 0$) sabitine sahip bir Tamamlayıcı Split Halka Rezonatör (CSRR) birim hücresidir. CSRR'ın etkisi Nicolson-Ross-Weir (NRW) yöntemini kullanarak simülasyon tabanlı saçılma parametreleri ile doğrulanmıştır. Sonuçlar permitivitenin, CSRR'nin rezonans frekansında negatif olduğunu göstermektedir.

Bu çalışma, geleneksel ve minyatür mikrostrip yama antenlerinin 5.15 GHz rezonans frekansındaki tasarımı ve simülasyonunu da sunmaktadır. İndirgeme oranı, CSRR aracılığıyla meta malzeme yapı uygulanarak % 80.7'e ulaşmaktadır. Bu antenler, Bilgisayar Simülasyon Teknolojisi Mikrodalga Stüdyosu (CST MWS) kullanılarak simüle edildi.

Anahtar Kelimeler: Meta Malzeme, CSRR Birim Hücre, geleneksel Mikroşerit Yama Anten, Minyatür Mikroşerit Yama Anten.

ACKNOWLEDGEMENT

All praise is due to Allah Subhanahu Wataala for his blessing and guidance**.** My immense gratitude goes to my supervisor, Asst. Prof. Dr. Rasime Uyguroğlu, for the patient, guidance, encouragement and advice she has provided throughout my time as her student. I feel extremely very lucky to have enjoyed the devotion to scrutinising my work and at the same time, promptly responding to my numerous questions. I am thankful for the support I received from all the members of Staff at the Department of Electrical and Electronics Engineering during period of my study.

I am deeply grateful for the support of my parents and wife, whose encouragement strengthens me always. I say a big thank you to my brother, my sisters and my children for understanding with me throughout this period.

To all my friends in LIBYA and TRNC, I am thankful for all the prayers, motivation and encouragement.

TABLE OF CONTENTS

ABSTRACT iii

ÖZ iv

ACKNOWLEDGEMENT v

LIST OF TABLES ix

LIST OF FIGURES x

LIST OF SYMBOLS AND ABBREVIATIONS xii

1 INTRODUCTION 1

1.1 Thesis Overview 1

1.2 Thesis Objective 2

1.3 Thesis Contributions 2

1.4 Thesis Outline 2

2 ANTENNA THEORY 4

2.1 Overview of Antennas 4

2.2 Parameters of Antennas 4

2.2.1 Antenna Gain 4

2.2.2 Radiation Pattern 5

2.2.3 Voltage Standing Wave Ratio (VSWR) 6

2.2.4 Return Loss (RL) 6

2.2.5 Bandwidth 6

2.2.6 Antenna Directivity 7

2.3 Definition of MPA 7

2.4 Advantages and Disadvantages of MPA 8

2.5 Types of MPA 9

2.6 Feeding Techniques of MPA.....9
2.6.1 Microstrip Line Feed.....10
2.7 Methods of Analysing MPA.....12
2.7.1 Transmission Line Method.....12
3 THEORY OF METAMATERIALS.....15
3.1 Metamaterials: A Review.....15
3.2 Materials Classification.....15
3.3 RHM and LHM from Maxwell's Equations.....17
3.4 Types of Metamaterials Structures.....19
3.4.1 SRR.....20
3.4.2 CSRR.....21
3.5 Measurement of Material Properties.....22
3.5.1 Nicholson-Ross-Weir (NRW).....23
4 ANTENNA DESIGNS AND RESULTS.....24
4.1 Introduction.....24
4.2 CMPA Design and Results.....25
4.2.1 CMPA Design.....25
4.2.2 CMPA Results.....26
4.3 MMPA Design and Results.....30
4.3.1 CSRR Unit Cell Design.....31
4.3.2 MMPA Design.....35
4.3.3 MMPA Results.....36
4.4 Results Discussion.....40
4.5 Antenna Design and Results of [6].....41
4.6 Comparison of Results.....43

5 CONCLUSION AND FUTURE WORK.....45

5.1 Conclusion.....45

5.2 Future Work.....45

REFERENCES.....46

LIST OF TABLES

Table 4.1: Parameters of CMPA.....26

Table 4.2: Optimized Parameters of CSRR Unit Cell Structure.....33

Table 4.3: Optimized Parameters of MMPA.....36

Table 4.4: Physical Parameters of Traditional and Miniaturized Antennas of [6] 42

Table 4.5: Comparison between Results of this Study and [6] 44

LIST OF FIGURES

Figure 2.1: 3D of a Radiation Pattern.....5

Figure 2.2: Bandwidth of an Antenna.....7

Figure 2.3: MPA Topology.....8

Figure 2.4: Patch Shapes (a) Rectangular (b) Square (c) Triangular (d) Circular.....9

Figure 2.5: Microstrip Line with Quarter Wave Impedance Transformer.....10

Figure 2.6: Microstrip Line with Inset Feed 11

Figure 2.10: Transmission Line Model.....12

Figure 2.11: Electric Field Lines.....13

Figure 2.12: Top View of Electric Field Lines.....14

Figure 3.1: Graph of Materials Classification.....16

Figure 3.2: Transverse Electromagnetic Wave in (a) RHM (b) LHM [14] 17

Figure 3.3: Different Metamaterials Structures (a) SRRs (b) Thin Wires (c) CSRRs (d) Slots Lines (LS).....19

Figure 3.4: Metamaterial with NIR.....20

Figure 3.5: Topology of SRR and Its Equivalent Circuit [15] 21

Figure 3.6: Topology of CSRR and Its Equivalent Circuit [15] 22

Figure 4.1: Topology of CMPA.....25

Figure 4.2: 3D CMPA Structure in CST.....26

Figure 4.3: Return Loss of CMPA.....27

Figure 4.4: 3D Gain of CMPA in dB.....28

Figure 4.5: Polar Plot of Antenna Gain of CMPA.....28

Figure 4.6: 3D Directivity of CMPA in dBi.....29

Figure 4.7: Polar Plot of Antenna Directivity of CMPA.....29

Figure 4.8: Topology of MMPA.....30

Figure 4.9: Flowchart of MMPA Design Methodology.....31

Figure 4.10: CSRR Unit Cell Structure.....32

Figure 4.11: CSRR Unit Cell Structure Embedded in a TEM Waveguide.....33

Figure 4.12: S-parameters of the Circular CSRR Unit Cell.....34

Figure 4.13: Real Values of Permittivity ε_r.....35

Figure 4.14: MMPA Structure in CST.....36

Figure 4.15: Return Loss of MMPA at Different CSRR Unit Cell Size.....37

Figure 4.16: Return Loss of MMPA.....38

Figure 4.17: 3D Gain of MMPA in dB.....38

Figure 4.18: Polar Plot of Antenna Gain of MMPA.....39

Figure 4.19: 3D Directivity of MMPA in dBi.....39

Figure 4.20: Polar Plot of Antenna Directivity of MMPA.....40

Figure 4.21: Return Loss of CMPA and MMPA.....40

Figure 4.22: 3D Structure of Miniaturized Antenna of [6] 41

Figure 4.23: Top View of Miniaturized Antenna with Physical Parameters of [6] ...42

Figure 4.24: Return loss of Traditional and Miniaturized Antennas of [6] 43

LIST OF SYMBOLS AND ABBREVIATIONS

a	Diameter of outer ring
$\vec{B}$	Magnetic Induction
Bw%	Bandwidth Efficiency
C	Light Speed
C	Space Ring Width
$\vec{D}$	Electric Displacement
$\vec{E}$	Electric Field
f_o	Operation Frequency
f_r	Resonant Frequency
$\vec{H}$	Magnetic Field
h	Substrate Thickness
L_{eff}	Effective Length of Patch
L_f	Microstrip Line Feed Length
L_P	Patch Length
L_s	Substrate Length
L_m	Metamaterial Length
RL	Return Loss
S11	Scattering Coefficients
S	Split Ring Width
W_f	Microstrip Line Feed Width
Wi	Inset Cut Width
W_p	Patch Width

W_s	Substrate Width
W_m	Metamaterial Width
ΔL	Increment Length
y_o	Inset Cut Length
Z_a	Antenna Impedance
Z_o	Microstrip Line Impedance
Z_t	Transformer Impedance
ε_r	Dielectric Permittivity
ε_{eff}	Effective Dielectric Permittivity
λ_c	Cut-off Wavelength
λ_c	Free Space Wavelength
Γ	Reflection coefficients
CMPA	Conventional Microstrip Patch Antenna
CSRR	Complementary Split Ring Resonator
CST	Computer Simulation Technology
DGS	Defected Ground Structure
DNG	Double Negative
DPS	Double Positive
ENG	Electric Negative
HFSS	High Frequency Structures Simulators
LHM	Left Handed Materials
MPA	Microstrip Patch Antenna
MMPA	Miniaturized Microstrip Patch Antenna
MNG	Magnetic Negative
PEC	Perfect Electric Conductor

PMC	Perfect Magnetic Conductor
RHM	Right Handed materials
SRR	Split Ring Resonator
VSWR	Voltage Standing Wave Ratio
Wi-Fi	Wireless Fidelity

Chapter 1

INTRODUCTION

1.1 Thesis Overview

Microstrip patch antenna (MPA) is the most common type of antennas, which is small size, low weight, little cost and easy manufacturing. Due to these attractive properties, MPA was used in many applications for wireless communications (like Bluetooth and Wi-MAX), and for military operations, it is also useful in the fabrication of radars. In recent years, the need of smaller size communication systems and small size antenna has continued to increase. Therefore, many different techniques have been used to minimize the size of MPA, like making slots in the radiation part [1] and using shorting posts [2], but these techniques are still unable to miniaturize the antenna to the desired size [3]. Research has revealed that is another technique which provides the easiest way to minimize the size of MPA, using a high permittivity substrate (ε) [4]. This method will reduce the size of MPA, but using this method lead to expensive cost and suffer from surface waves which degrade the radiation pattern of MPA by increasing the amount of side lobes significantly [5]. Therefore, it was necessary to find a way to reduce the size of MPA without affecting its inherent characteristics.

Researchers tend to use metamaterials substrate to reduce the size of MPA and improve their performance [6]. Metamaterials are artificial structures which have electromagnetic properties that do not exist in the real nature. In the past,

metamaterials were categorized as a structure or designs that have simultaneously negative permeability and permittivity. In current study, CSRR unit cell which has negative permittivity (ε) and positive permeability (μ) is used to miniaturize MPA. Miniaturization design consists of two separate substrates, the CSRR plane is sandwiched in between them. The patch antenna is on the top and ground plane in the bottom of the structure.

1.2 Thesis Objective

The objective of this thesis is to design and simulate MPA to achieve size reduction by using the unique properties of metamaterials via CSRR unit cell in the substrate.

1.3 Thesis Contributions

In this thesis, the patch size of conventional microstrip patch antenna is reduced from 249.6 mm to 49 mm in miniaturized microstrip patch antenna at the resonant frequency of 5.15 GHz.

1.4 Thesis Outline

This thesis is organized into five chapters. Basically, the first chapter lays a background upon which the other four chapters built upon.

In Chapter 2, effort is made to discuss the general theory, antenna parameters, feeding types and parameters of microstrip patch antennas respectively.

Chapter 3 presents the definition and historical view of metamaterials, the general theory of different materials based on sign of permittivity (ε_r) and permeability (μ_r) by explaining the Maxwell's equations, types of metamaterials structures. For example, split ring resonators (SRR) and CSRR, measurement of material properties

by using Nicolson-Ross-Weir (NWR) method to calculate permittivity (ε_r) and permeability (μ_r) properties.

In chapter 4, design and simulation results of CMPA at 5.15 GHz are presented, using the CST software. For the design and simulation results of CSRR unit cell at 5.15 GHZ, the CST software is also used. The design and simulation results of MMPA at 5.15 GHZ by using CST software are presented.

While in Chapter 5, the conclusions and suggested areas for possible future research are outlined.

Chapter 2

ANTENNA THEORY

2.1 Overview of Antennas

In general, antennas are metallic structures that radiate and receive electromagnetic waves. The first experiment of antenna was done by the German physicist, Heinrich Rudolf Hertz in 1887 [7]. After that, antennas were developed by many other scientists during the last century. Today, we have various types of antennas, which have different structures and characteristics such as:

1- Wire Antennas

2 - Aperture Antennas

3 – Microstrip Patch Antennas

4 - Array Antennas

5 - Reflector Antennas

6 - Lens Antennas

2.2 Parameters of Antennas

Any type of antenna has various parameters that determine the eventual quality outcome. In various cases, some of the parameters need improvement and very common examples are gain and bandwidth

2.2.1 Antenna Gain

Antenna gain is known as rate of the intensity, in a given direction, to the radiation intensity that would be obtained if the power accepted by the antenna was radiated isotropically. It describes how the antenna converts input power into radio waves to

specified direction in a transmitting antenna that is called antenna's directivity. Also, it describes how the antenna converts radio waves, which arrive from specified direction into electrical power in a receiving antenna known as electrical efficiency.

2.2.2 Radiation Pattern

The radiation pattern of an antenna is a plot of the far-field radiation from the antenna. In general, the radiation pattern is a plot of the power radiated from an antenna per unit solid angle (θ) or its radiation intensity ($\cup$). This pattern is divided into three lobes: the main lobe is the radiation lobe in the maximum direction of the radiation; the back lobe is the minor lobe, which is opposite to the main lobe; while side lobes are the minor lobes between the main lobe and the back lobe. Figure 2.1 shows a radiation pattern.

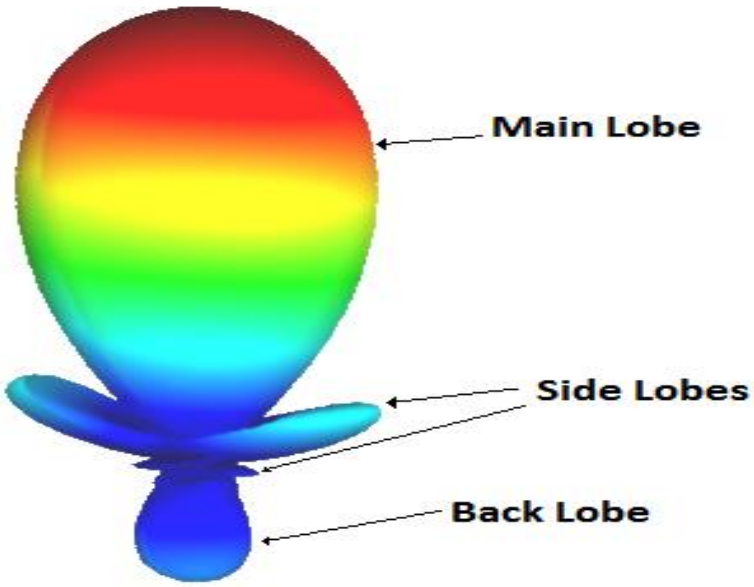

Figure 2.1: 3D of a Radiation Pattern

2.2.3 Voltage Standing Wave Ratio (VSWR)

(VSWR) is defined as function of reflection coefficient, which describes the power reflected from the antenna. VSWR is given by equation 2.1 below.

$$\text{VSWR} = \frac{1+|\Gamma|}{1-|\Gamma|} \tag{2.1}$$

VSWR is always larger than l.0 and a positive number. The smallest value of VSWR (VSWR=1.0), means the antenna is matched to the transmission line, where all power is delivered to the antenna and no power is reflected, then the case is in an ideal form. The highest acceptable value of VSWR is 2.0 and that means the antenna is matched with reflected power to the source, and this case is the worst situation to match. When the value of VSWR is more than 2.0, it means all power is reflected to the source and no power is delivered and this case is mismatching.

2.2.4 Return Loss (RL)

The return loss (S-parameter) is the loss of the input power in transmitted signal due to input impedance and is given by equation 2.2 as follows.

$$\text{RL} = -20\log|\Gamma| \tag{2.2}$$

2.2.5 Bandwidth

Another parameter of antennas is the bandwidth (BW). The bandwidth is known as the frequency range (in terms of performance of the antenna) with respect to some characteristics conforming to a specific standard. Figure 2.2 below shows bandwidth of an antenna.

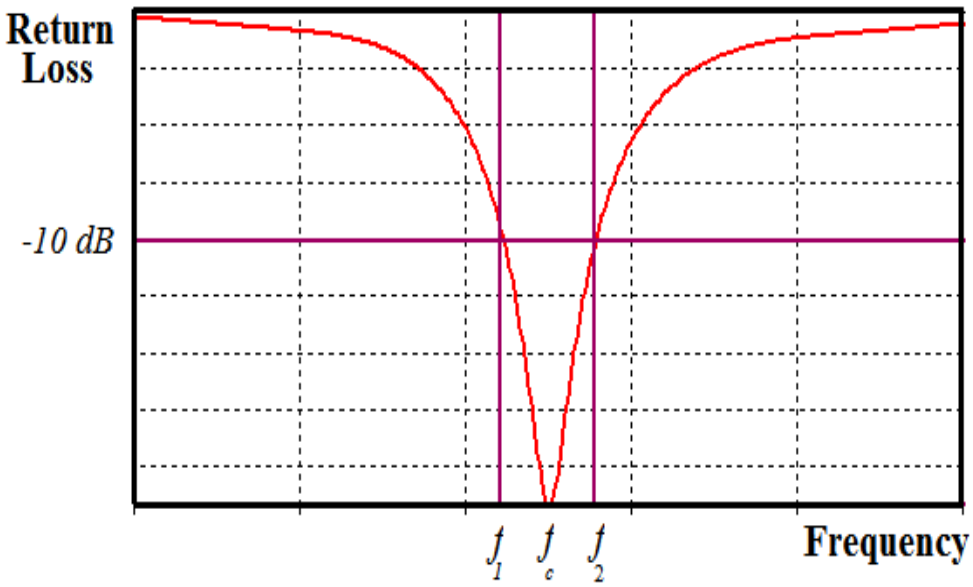

Figure 2.2: Bandwidth of an Antenna

The bandwidth efficiency is determined by equation 2.3 below.

$$BW\% = \frac{f_2 - f_1}{f_c} \times 100 \tag{2.3}$$

2.2.6 Antenna Directivity

The directivity of an antenna is the rate of radiation intensity in a given direction to the radiation intensity that would be obtained if the total power radiated by the antenna were to be radiated isotropically.

2.3 Definition of MPA

Historical account reveals that in year 1950, was when the first MPA appeared. Then it took about twenty years for it to take the ideal form [9]. Today, MPA is the most useful antenna which operates at high frequency (f > 1 GHz). MPA consists of three layers: the radiation part (which is called patch), dielectric material (which is called substrate) and ground plane. The topology of MPA is shown in figure 2.3.

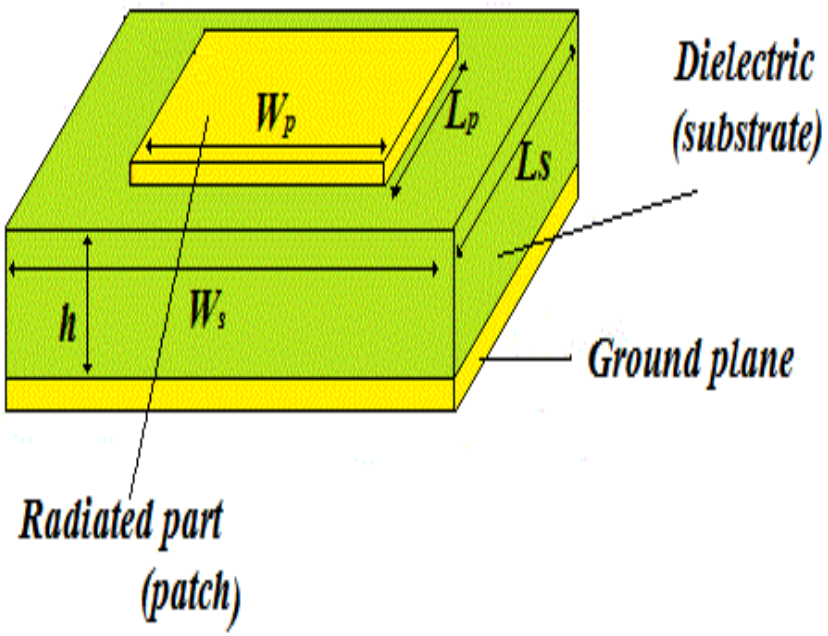

Figure 2.3: MPA Topology

The patch and ground plane are made from conducting materials such as copper. The substrate made from a poor conductor of electricity material. The substrate has a big effect on the resonant frequency (f_r) and the bandwidth BW. When there is increase or decrease in the relative permittivity constant ε_r of the substrate, the resonant frequency f_r will change. In addition, the substrate is also able to control the bandwidth (BW) of the antenna by increasing or decreasing the thickness of the substrate (h).

2.4 Advantages and Disadvantages of MPA

The most notable advantages of MPA are that it comes in small sizes, has low profile, has light weight and tend to be conformable on planar and non-planar surfaces. However, there are some disadvantages of MPA. The main disadvantages are the low efficiency and narrow bandwidth of less than 6%.

2.5 Types of MPA

The patch antennas may have different patch shapes which have been designed to match specific characteristics. Figure 2.4 shows the some of the common types of patches are rectangular, square, triangular and circular patches. Whereas, the substrate and ground plane always have rectangular or square form in general.

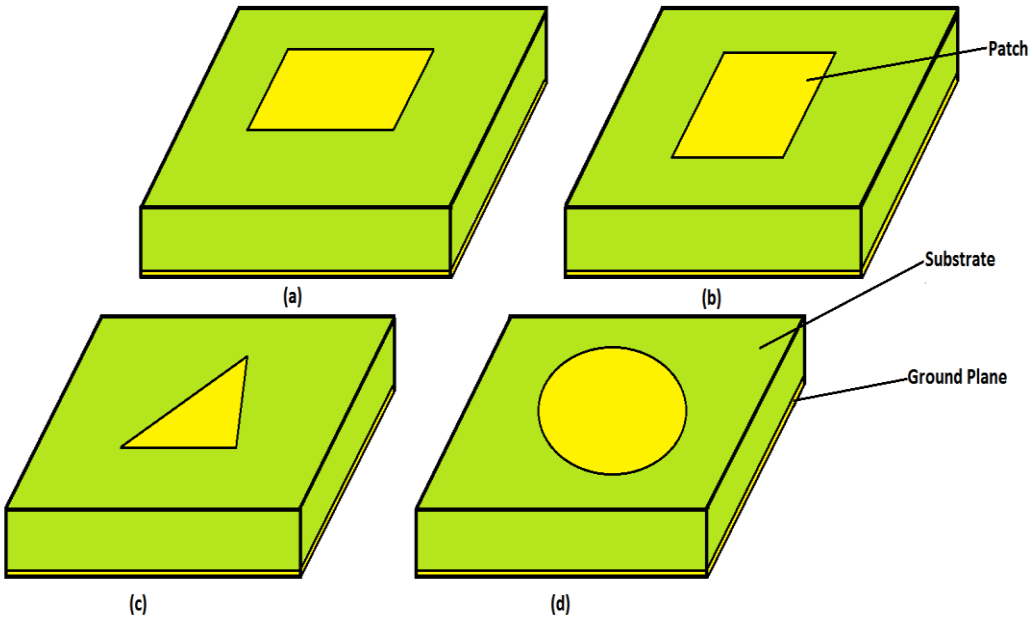

Figure 2.4: Patch Shapes (a) Rectangular (b) Square (c) Triangular (d) Circular

2.6 Feeding Techniques of MPA

There are mainly four methods for feeding the MPA. These are:

1. Microstrip line feed.

2. Coaxial feed.

3. Proximity coupling feed.

4. Aperture coupling feed.

In this study, microstrip line feed is used because of its advantages.

2.6.1 Microstrip Line Feed

This type of feed technique is a strip line feed is linked directly to the edge of the patch. This method is very simple to design and fabricate. In addition, the strip line feed is etched on the same substrate to supply a planar structure. However, this technique has some limitations. If thickness of the substrate rises, then the surface waves and the spurious radiation also will increase. There are two ways to connect microstrip line feed with the patch. The first way is using a quarter wave transformer impedance (Z_t) to matching a microstrip line impedance (Z_o) 50 Ω with the patch antenna impedance (Z_a). As represented in the figure 2.5 below.

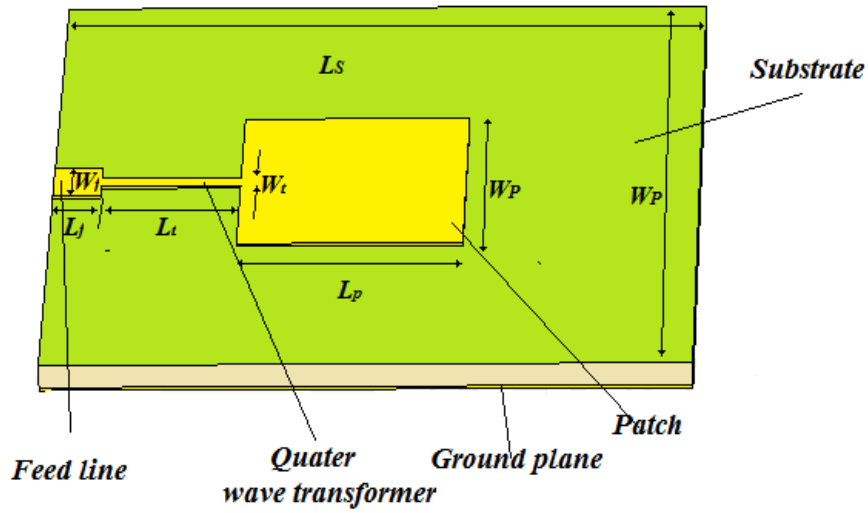

Figure 2.5: Microstrip Line with Quarter Wave Impedance Transformer

The value of the quarter wave transformer impedance (Z_t) is given by equation 2.4.

$$Z_t = \sqrt{z_a z_o} \tag{2.4}$$

Where the microstrip line impedance Z_o always is equal 50 Ω.

The antenna impedance Z_a could be found by equations 2.5 if ($\frac{w_p}{h} > h$).

$$Z_a = \frac{120\pi}{\sqrt{\varepsilon_{eff}}}\left[\frac{w}{h} + 1.393 + 0.667 \ln\left[\frac{w_p}{h} + 1.444\right]\right] \quad (2.5)$$

When ($\frac{w_p}{h} < h$) the antenna impedance $Z_a$is calculated by equation 2.6.

$$Z_a = \frac{60}{\sqrt{\varepsilon_{eff}}} \ln\left[\frac{8h}{w_p} + \frac{w_p}{4h}\right] \quad (2.6)$$

The second way is the inset feed in the patch to achieve 50-Ω input impedance. The useful of the inset feed in the patch is to connect the impedance of the feed line to the patch input impedance without the need for any additional connecting element as illustrated in the figure 2.6 below.

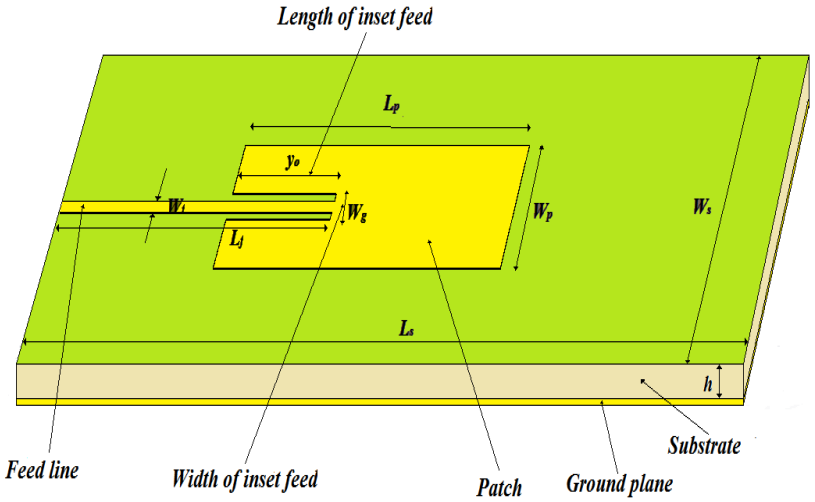

Figure 2.6: Microstrip Line with Inset Feed

The width of inset cut is optimized, whereas, the length of inset cut (y_o)is calculated in equation 2.7below[8].

$$y_o = 10^{-4}[0.001699\varepsilon_r^7 + 0.1376\varepsilon_r^6 - 6.1783\varepsilon_r^5 + 93.187\varepsilon_r^4 - 682.69\varepsilon_r^3 + 256.9\varepsilon_r^2 - 4043\varepsilon_r + 6697]\,\frac{L_p}{2} \quad (2.7)$$

2.7 Methods of Analysing MPA

There are many methods which are used to analyse MPA. For instance, the transmission line method, cavity method, wire grid method, integral equation method, vector potential approach, dyadic green's function technique and radiating aperture method. However, the transmission line method is selected for discussion in this chapter.

2.7.1 Transmission Line Method

The transmission line method is one of the most famous methods used to analyze the MPA. This model is illustrated in figure 2.7 below.

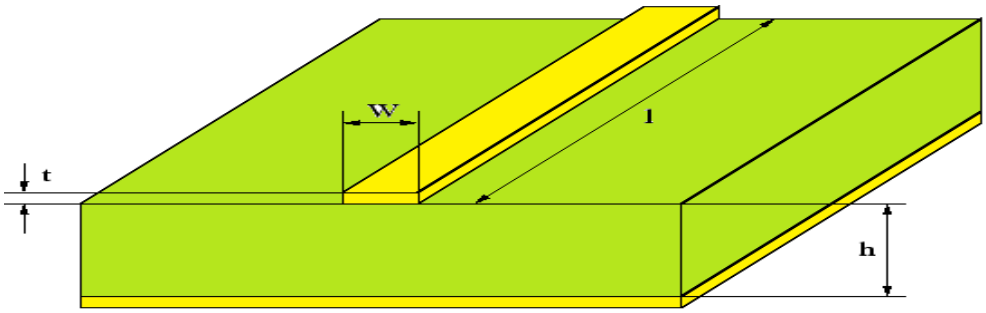

Figure 2.7: Transmission Line Model

Generally, the transmission line method is considered the simplest way to study MPA and it has two different cases. The first case is (w/h) < 1 (narrow strip line), but this case is not important to apply on microstrip antenna. The second case is (w/h) >1 (wider strip line), which is more common than the first case and is used here to explain the characteristics of the MPA.

In this method, transmission line model equations are used to design MPA. The first step to design MPA is to select the type of substrate and operating frequency (f_o).

The second step is calculating the suitable thickness of the dielectric substrate (h) as given in the equation below.

$$h \leq \frac{0.3\ c}{2\pi f_0 \sqrt{\varepsilon_r}} \tag{2.8}$$

Where, h is height of dielectric substrate, c is the speed of light 3×10^8 m/s and (ε_r) is the electrical permittivity of the dielectric substrate.

The third step is to find the width (w_p) of the patch antenna by using formula 2.9 below.

$$w_p = \frac{c}{2f_o\sqrt{\frac{\varepsilon r+1}{2}}} \tag{2.9}$$

The fourth step is to calculate the effective of dielectric constant (ε_{eff}). Due to move the electric field lines via the vacuum before passing throe the substrate as shown in figure 2.8 below.

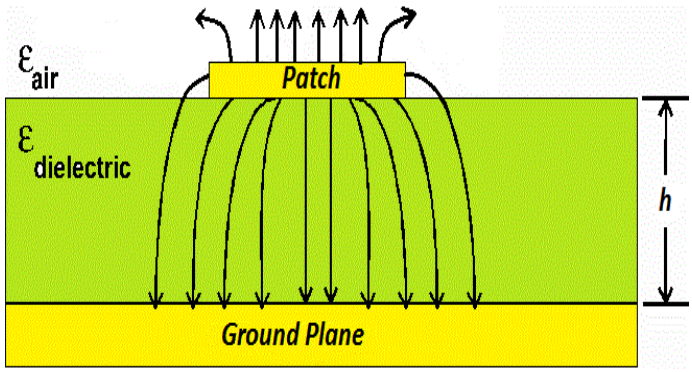

Figure 2.8: Electric Field Lines

The effective of dielectric constant ε_{eff} is given by formula 2.10.

$$\varepsilon_{eff} = \frac{\varepsilon_r+1}{2} + \frac{\varepsilon_r-1}{2}\left[1+12\frac{w_p}{h}\right]^{\frac{1}{2}} \tag{2.10}$$

The fifth step is to calculate the length of the patch antenna (L_p) as given in formula 2.11.

$$L_p = L_{eff} - 2\Delta L \tag{2.11}$$

Where, L_{eff} is the effective length, which occurs because of the electric filed lines movement as shown in figure 2.9 below.

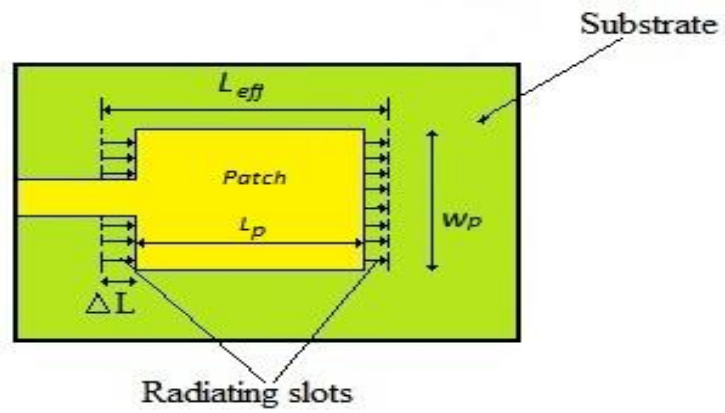

Figure 2.9: Top View of Electric Field Lines

The effective length can be calculated from equation 2.12.

$$L_{eff} = \frac{c}{2 f_o \sqrt{\varepsilon_{eff}}} \tag{2.12}$$

The change of length *(ΔL)* can be calculated from equation 2.13 below.

$$\Delta L = 0.412h \frac{(\varepsilon_{eff} + 0.3)\ (\frac{w_p}{h} + 0.264)}{(\varepsilon_{eff} - 0.264)\ (\frac{w_p}{h} + 0.8)} \tag{2.13}$$

The sixth step is to calculate the width and the length of the substrate by using equations 2.14 and 2.15 respectively.

$$Ws \geq w_p + 6*h \tag{2.14}$$

$$Ls \geq L_p + 6*h \tag{2.15}$$

Chapter 3

THEORY OF METAMATERIALS

3.1 Metamaterials: A Review

Metamaterials are artificial materials having negative value of relative permittivity **(**ε<0**)** and permeability (μ<0), which are not available in nature. Metamaterials became the one of the hottest topics in microwave applications during the last years due to their rare properties which are absent in nature. The most famous application of metamaterials in microwave, is their use in microstrip patch antennas to improve antenna performance or reduction in antenna size [9][3]. The word metamaterial was proposed by Rodger M. Wasler of University of Taxas. The root of the word "meta" is Greek, and it means beyond, which in its real sense, metamaterial means beyond the material [10]. In 1967, a Russian Physicist Viktor Veselago, was the first to study the electrodynamics of substances with simultaneously negative values of dielectric permittivity (ε) and magnetic permeability (μ) [11]. Later in year 2000, precisely 33 years on, Dr. Smith and his colleagues conducted the first experiment to achieve negative permittivity **(**ε**)** and negative permeability (μ***)*** when they designed thin wire (TW) (that shows the negative permittivity) and SRR structure (that shows the negative permeability) [12].

3.2 Materials Classification

The materials are divided into four types based on values of permeability and permittivity [13].

The first type is the conventional material, which has double positive structure (DPS) ($\mu>0$) and ($\varepsilon > 0$). These are the basic properties available in nature called Right Handed Materials (RHM).

The second type has ($\varepsilon< 0$) and ($\mu > 0$) value (ENG). These materials show the class of metamaterials are defined as artificial dielectrics. Due to its highly negative dielectric value, these type of metamaterials can be able to reduce the size of MPA.

The third type shows the materials with ($\varepsilon> 0$) and ($\mu < 0$) value (MNG). This class of metamaterials is called artificial magnetic. These type of metamaterials can be able to increase the gain.

The last type has Double Negative (DNG) permeability and permittivity ($\mu<0$), and ($\varepsilon < 0$). This class of metamaterials is called Left Handed Materials (LHM) because it has backward waves propagation. Figure 3.1 below illustrates materials classification.

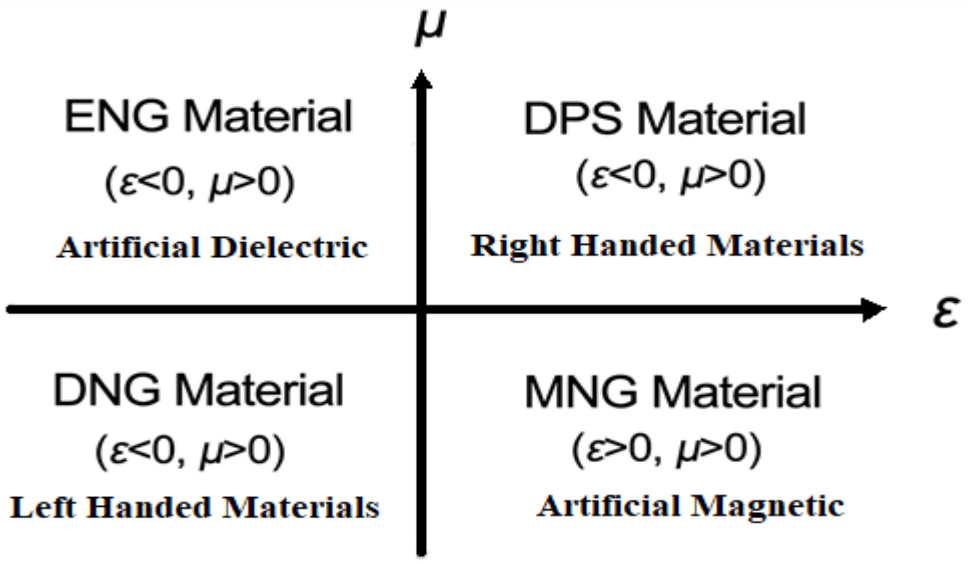

Figure 3.1: Graph of Materials Classification

3.3 RHM and LHM from Maxwell's Equations

The electromagnetic properties of the materials (that is, the relative permittivity and permeability) determine the direction to which the electromagnetic waves propagate through a material. Maxwell's equations can explain the direction of the electromagnetic wave propagation through various media.

The first condition where a materiel has positive sign of (ε) and (μ) is normal situation and the electromagnetic waves travel from left to right as shown in figure 3.2 (a). The second condition when the sign of (ε) and (μ) is different, therefore, the electromagnetic waves cannot be propagated and they are attenuated. The last condition when material has negative sign of (ε) and (μ), the electromagnetic waves travel from right to left as Veselago predicted as illustrated in figure 3.2 (b).

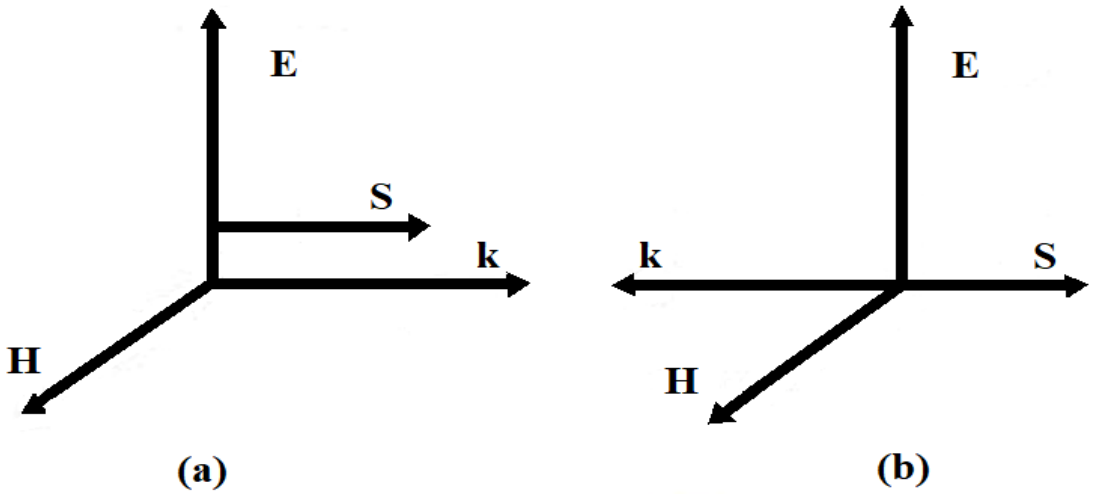

Figure 3.2: Transverse Electromagnetic Wave in (a) RHM (b) LHM [13]

The Maxwell's equations are;

$$\nabla \times \vec{E} = -\frac{\partial B}{\partial t} \tag{3.1}$$

$$\nabla \times \vec{H} = \frac{\partial D}{\partial t} \tag{3.2}$$

$$\vec{B} = \mu \vec{H} \tag{3.3}$$

$$\vec{D} = \varepsilon \vec{E} \tag{3.4}$$

From these equations, we can conclude the equations of propagation of electromagnetic waves for conventional material DPS are given in equations 3.5, 3.6.

$$\vec{k} \times \vec{E} = \omega \mu \vec{H} \tag{3.5}$$

$$\vec{k} \times \vec{H} = -\omega \varepsilon \vec{E} \tag{3.6}$$

Where $(\overrightarrow{k})$ is propagation constant, (ω) is the angular frequency.

The equations of propagation of electromagnetic waves for metamaterials DNG are given in equations 3.7, 3.8.

$$\vec{k} \times \vec{E} = -\omega \mu \vec{H} \tag{3.7}$$

$$\vec{k} \times \vec{H} = \omega \varepsilon \vec{E} \tag{3.8}$$

Energy flow is determined by the real part of the Poynting vector $(\vec{S})$ as shown in equation 3.9 below.

$$\vec{S} = \frac{1}{2}[\overrightarrow{E} \times \vec{H}^*] \tag{3.9}$$

The propagation constant (k) is given by equation 3.10 below.

$$k^2 = \frac{\omega^2}{c^2} n^2 \tag{3.10}$$

For simultaneous change of sign of (ε) and (μ), the direction of energy flow is not affected, therefore, the group velocity is positive for both LHM and RHM. Refractive index is given by equation 3.11 and the phase velocity is given by equation 3.12 below.

$$n = \pm \sqrt{\varepsilon \mu} \tag{3.11}$$

$$v_p = \frac{c}{n} \tag{3.12}$$

3.4 Types of Metamaterials Structures

Metamaterials are artificially produced structures, having negative permittivity ε and permeability μ values. There are four basic metamaterials structures that are based on the values of permittivity and permeability. SRR and slot structures have (μ< 0) and (ε> 0). CSRR and TW structures have (μ>0) and (ε<0). Figure 3.4 below shows the most common structures of metamaterials used in microwave area.

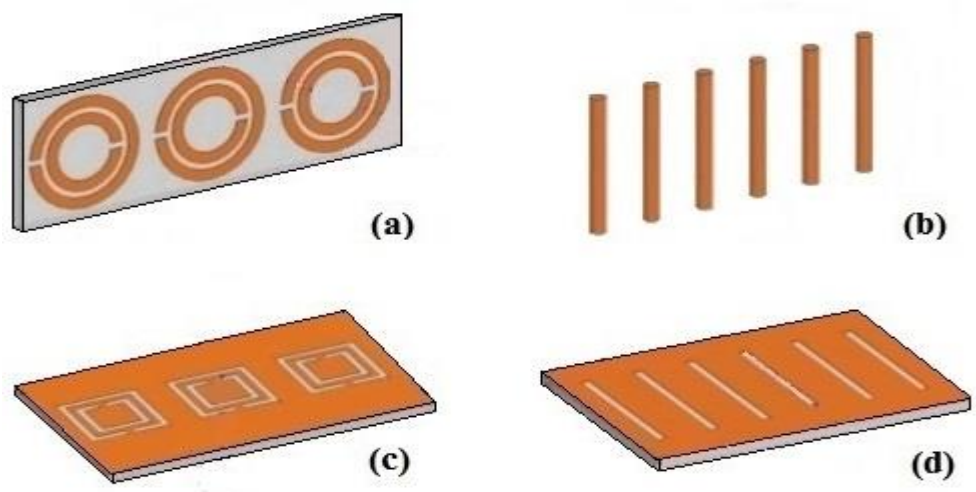

Figure 3.3: Different Metamaterials Structures (a) SRRs (b) Thin Wires (c) CSRRs (d) Slots Lines (LS)

left-handed metamaterials, which have double negative ($\mu<0$) and ($\varepsilon<0$) made from two metamaterials structures MNG (negative permeability) and ENG (negative permeability) are companied together in one structure. The structure composed of SRR and TW was designed by Dr. Smith and his colleagues in 2000, has negative permittivity $\boldsymbol{\varepsilon}$ and negative permeability μ [12]. Figure 3.4 shows metamaterials with Negative Index of Refraction (NIR).

Figure 3.4: Metamaterials with NIR

Clearly, there has been several debates about the SRR and CSRR structures during the last years by researchers around the world.

3.4.1 SRR

The first appearance for SRR was in 1999 by Prof. Pendry when he made two split rings, which was printed on a substrate [14]. The rings are made of non-magnetic metal like copper and have a small gap between them. SRR has ($\mu<0$) and ($\varepsilon>0$), therefore, it is called artificial magnetic MNG. Topology of the SRR and its equivalent-circuit model are shown in figure 3.5.

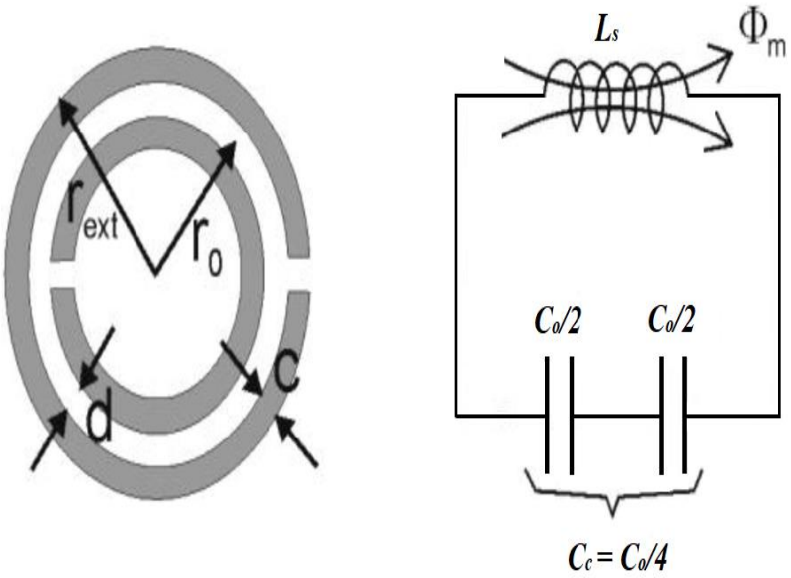

Figure 3.5: Topology of SRR and Its Equivalent Circuit [15]

From figure 3.5 the resonant frequency for SRR is given by equation 3.14 below.

$$f_r = \frac{1}{2\pi\sqrt{L_S C_S}} \tag{3.14}$$

3.4.2 CSRR

CSRR was made by Falcone in 2004, as new material has ($\varepsilon<0$) and ($\mu>0$) [16]. CSRR structure, considered being a negative image of an SRR, may be used on the ground plane of substrate, on the radiation patch or as a unit cell in the substrate. There are many shapes for CSRR but circular shape and square shape are the most famous designs. Sometimes, CSRR has more than one ring. The number of rings and their sizes have a big effect on resonant frequency of CSRR. Figure 3.6 illustrates the topology of CSRR and its equivalent circuit.

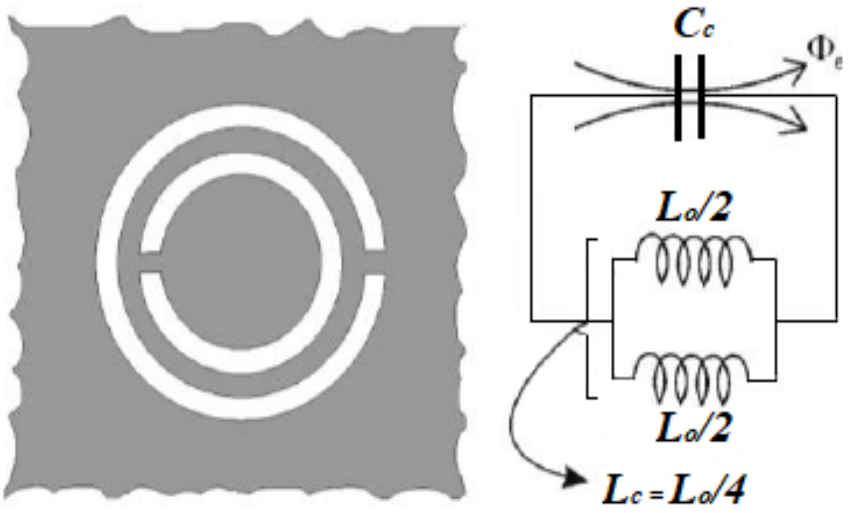

Figure 3.6: Topology of CSRR and Its Equivalent Circuit [15]

By the analysis of the equivalent circuit of CSRR, resonant frequency is given by equation 3.15.

$$f_r = \frac{1}{2\pi\sqrt{L_c C_c}} \tag{3.15}$$

3.5 Measurement of Material Properties

Many methods have been used to measure (**ε)** and (μ) such as techniques in time domain or frequency domain. The methods are used to convert from S-parameter to permittivity (ε_r) and permeability (μ_r) properties. Some of these methods are:

1 - Nicolson-Ross-Weir method

2 - NIST iterative method

3 - New non-iterative method

4 - Short circuit line method

In this section, the Nicolson-Ross-Weir method is considered for the calculation of permittivity (ε_r) and permeability (μ_r).

3.5.1 Nicholson-Ross-Weir (NRW)

NRW is the most popular method which use to calculate of both the (ε) and (μ) from the S-parameters [17]. The reflection coefficient is given by equation 3.16 below.

$$\Gamma = x \mp \sqrt{x^2 - 1} \tag{3.16}$$

From (S_{11},S_{21})taken from the simulation results, one can calculate (x) as given in equation 3.17 below.

$$x = \frac{S_{11}^2 - S_{21}^2 + 1}{2S_{11}} \tag{3.17}$$

The transmission coefficient is calculated by equation 3.18 below.

$$T = \frac{S_{11} + S_{21} - \Gamma}{1 - (S_{11} + S_{21})\Gamma} \tag{3.18}$$

The permeability (μ_r) is given by equation 3.19 below.

$$\mu_r = \frac{1+\Gamma}{\Lambda(1-\Gamma)\sqrt{\frac{1}{\lambda_0^2} - \frac{1}{\lambda_c^2}}} \tag{3.19}$$

$$\frac{1}{\Lambda^2} = -\left[\frac{1}{2\pi L} Ln\left(\frac{1}{T}\right)\right]^2 \tag{3.20}$$

The permittivity (ε_r) is given by equation 3.21.

$$\varepsilon_r = \frac{\lambda_0^2}{\mu_r}\left[\frac{1}{\lambda_c^2} + \frac{1}{\Lambda^2}\right] \tag{3.21}$$

Chapter 4

ANTENNA DESIGNS AND RESULTS

4.1 Introduction

This chapter illustrates the design and simulation results for CMPA and MMPA. CMPA and MMPA are designed at operation frequency of 5.15GHz. CSRR unit cell is used to reduce the size of CMPA.

In general, there are three different methods of CSRR that are used with CMPA. The first method is called Defected Ground Structure (DGS) [18]. DGS can reduce the size of the CMPA but this has some limitations as decreasing the front to back ratio of the radiation pattern. The second method is etched CSRR in the patch, this method cannot reduce the size of CMPA but it is commonly used to get better the performance of CMPA [9]. The third method is the structure obtained by placing the CSRR metamaterial unit cell in substrate or between two substrates [6] [19]. In this study, the CSRR metamaterial unit cell in substrate is utilized to miniaturize the size of CMPA. Results of the traditional microstrip patch antenna and miniaturized microstrip patch antenna of [6] and CMPA and MMPA introduced in this study will be compared. Computer Simulation Technology Microwave Studio (CST MWS) is used in this study.

4.2 CMPA Design and Results

4.2.1 CMPA Design

The CMPA consisting of three layers of square patch made from copper, Rogers RT6002 (lossy) substrate which has permittivity ε_r= 2.92 and square ground plane made from copper as shown in figure 4.1 below.

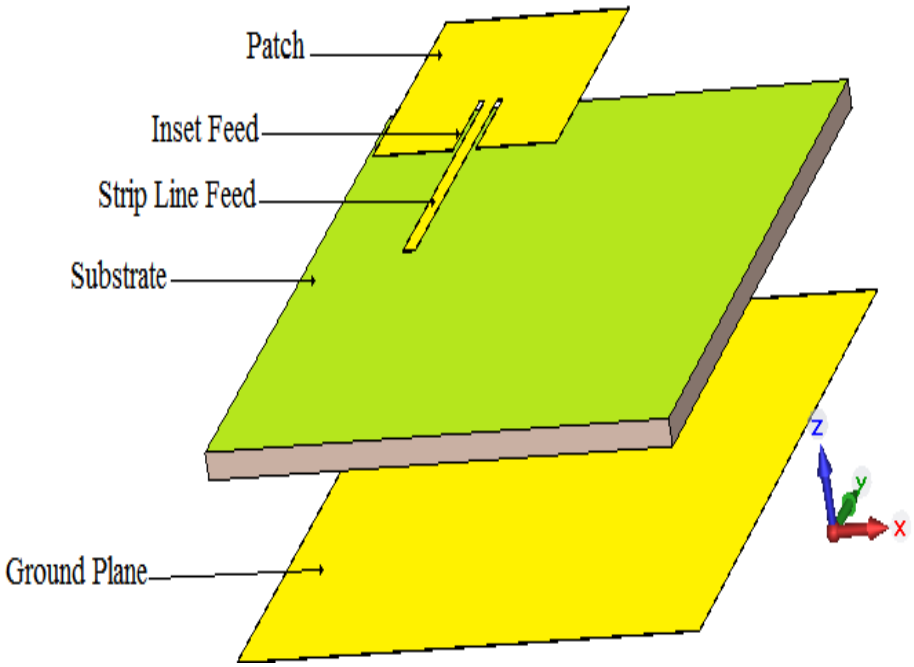

Figure 4.1: Topology of CMPA

Microstrip feed line with (W_f) as width and (L_f) as length is considered. connecting between the patch and the microstrip feed line, is achieved by the inset cut with cut length (y_o) and cut width (Wg). The first step of CMPA is to select the operation frequency $f_o = 5.15$ GHz, permittivity $\varepsilon_r = 2.92$ and the thickness of substrate h=1.524 mm. By applying the equations of MPA, all parameters of CMPA are illustrated in table 4.1.

Table 4.1: Parameters of CMPA

Parameters of the antenna	**Definition of the parameter**	**Value of parameter mm**
Ws	Substrate width	40
Ls	Substrate length	40
Wp	Patch width	15.95
Lp	Patch length	15.95
Wf	Feed line width	1.095
Lf	Feed line length	15.28
Wg	Inset cut width	2
y_o	Inset cut length	5.8
t	Patch thickness	0.035

4.2.2 CMPA Results

After calculating the parameters of CMPA, the design is simulated by using the microwave simulation software CST. Figure 4.2 below shows the 3D design structure of CMPA in CST.

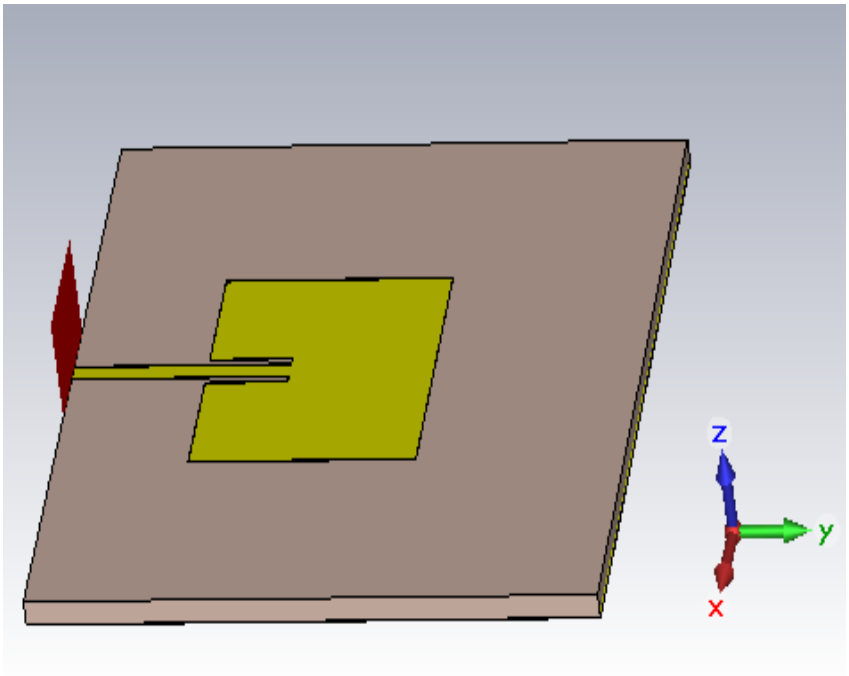

Figure 4.2: 3D CMPA Structure in CST

The simulation process demonstrates that return loss of CMPA was -25.004 dB at resonant frequency 5.15 GHz and the bandwidth efficiency of the CMPA at -10 dB is 2.3 %. Figure 4.3 below illustrates return loss of CMPA.

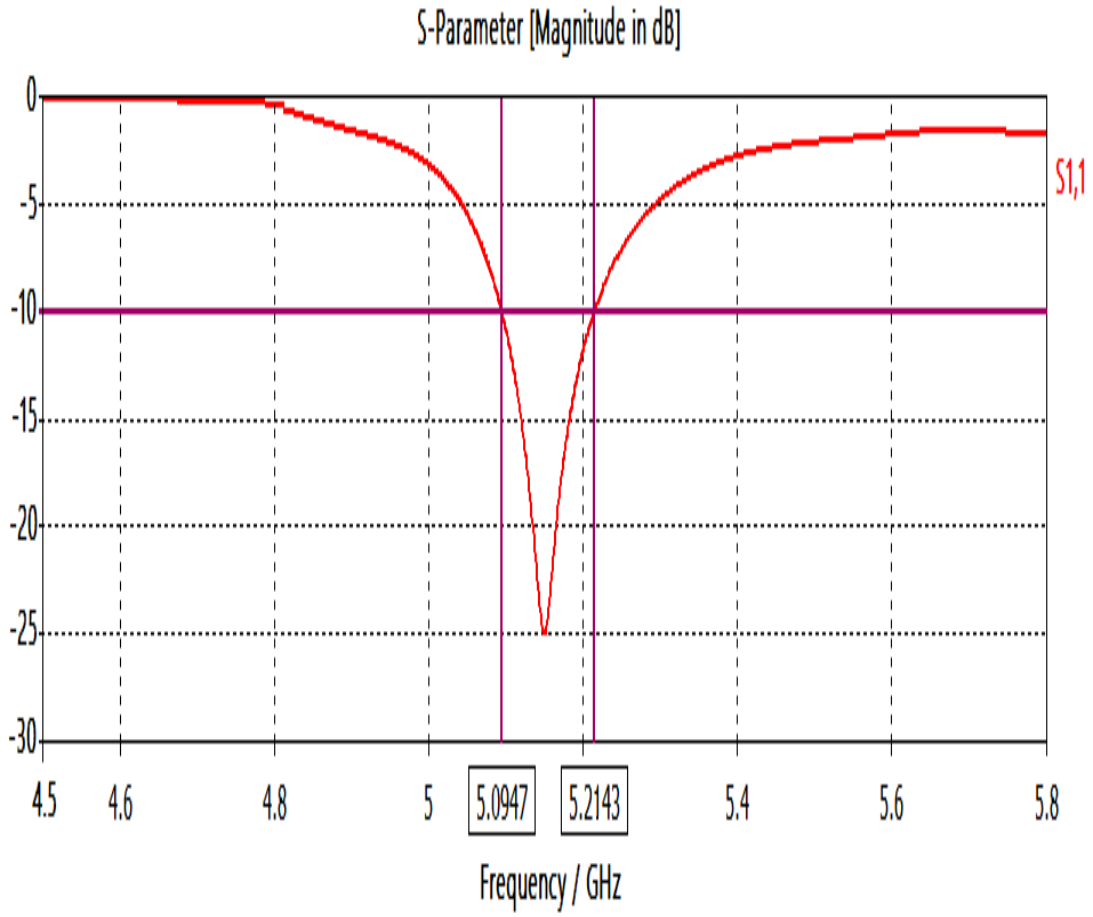

Figure 4.3: Return Loss of the CMPA

The antenna gain of CMPA is 7.22 dB as illustrated in figures 4.4 and 4.5 below.

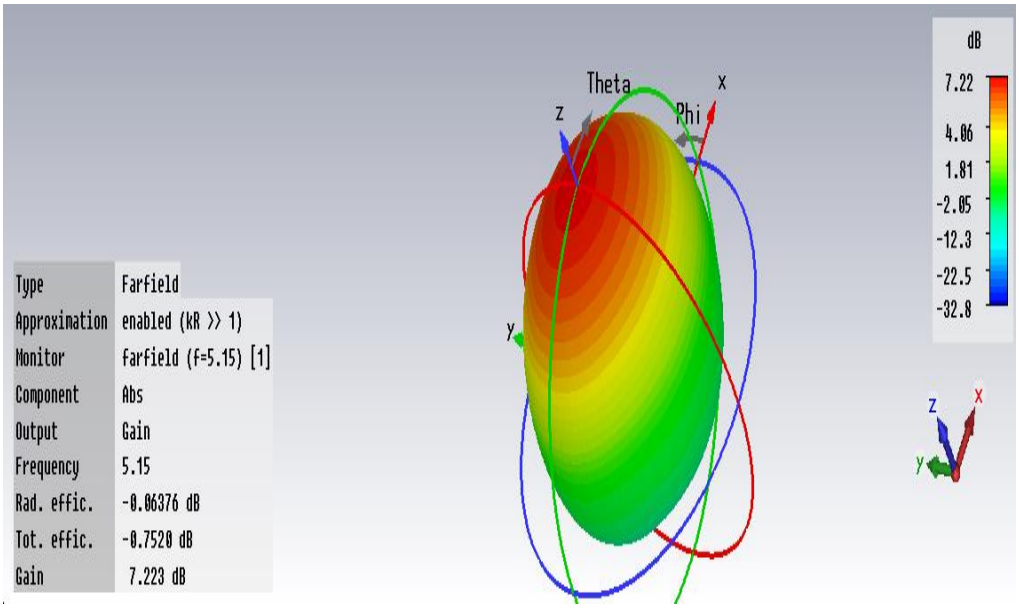

Figure 4.4: 3D Gain of CMPA in dB

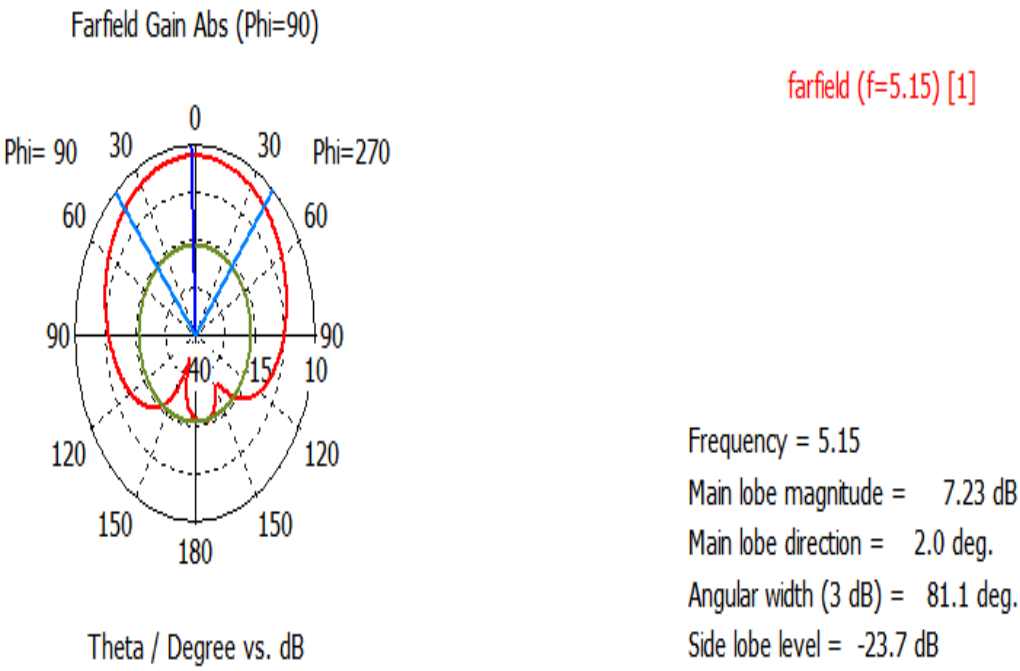

Figure 4.5: Polar Plot of Antenna Gain of CMPA

The antenna directivity of the CMPA is 7.29 dBi as shown in figures 4.6 and 4.7 below.

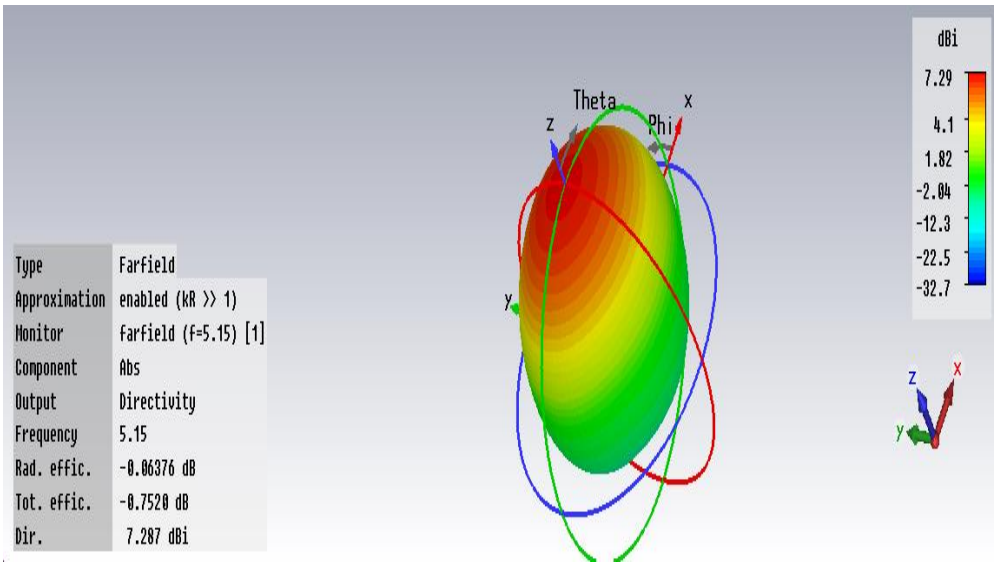

Figure 4.6: 3D Directivity of CMPA in dBi

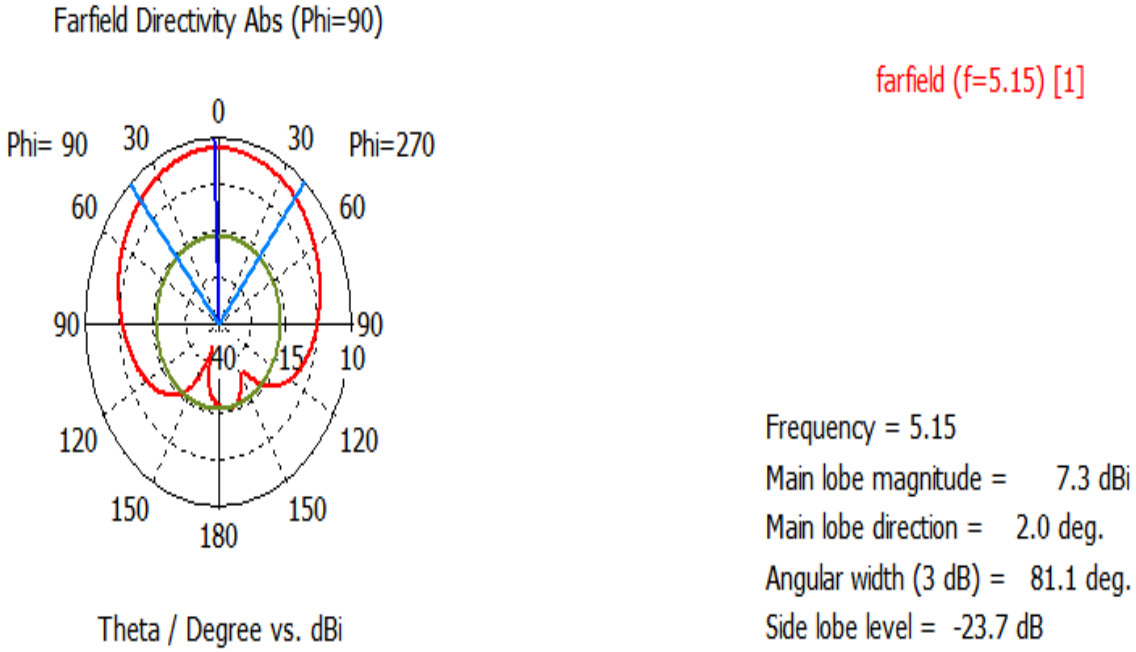

Figure 4.7: Polar Plot of Antenna Directivity of CMPA

4.3 MMPA Design and Results

The MMPA has CSRR unit cell which is placed in between two separate substrates, while a patch is printed on the surface of the top plane, and the ground is printed on the surface of the bottom plane. Figure 4.8 shows topology of MMPA.

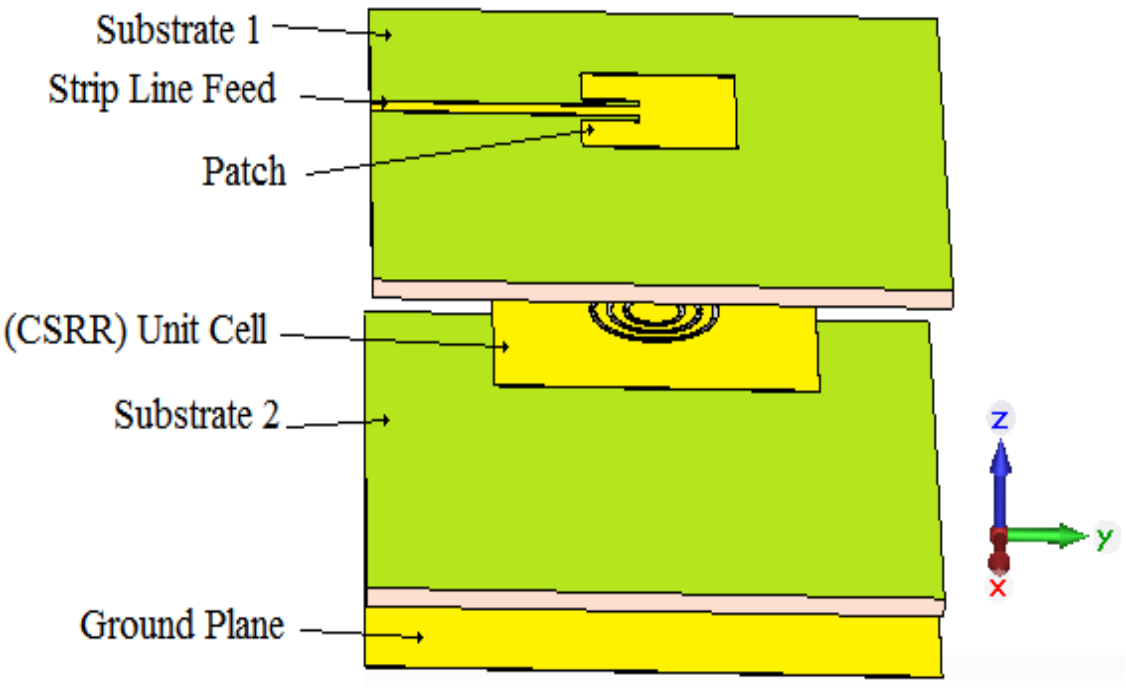

Figure 4.8: Topology of MMPA

The design methodology of MMPA is divided into two parts. First, the design of CSRR unit cell at resonant frequency 5.15 GHz and then the design of MMPA. Figure 4.9 illustrates the flowchart of MMPA design methodology.

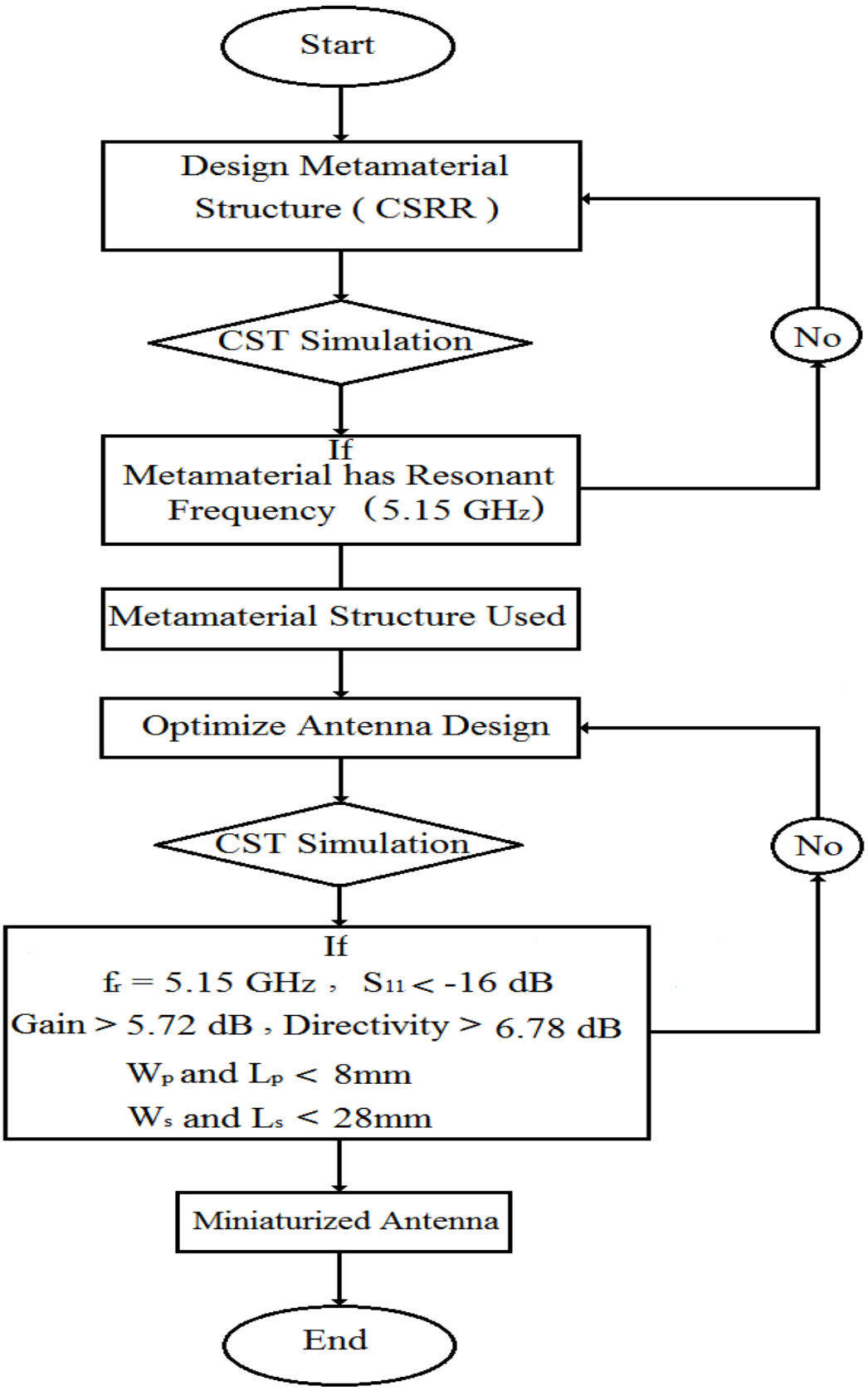

Figure 4.9: Flowchart of MMPA Design Methodology

4.3.1 CSRR Unit Cell Design

Before designing MMPA, CSRR unit cell was designed. Design of the CSRR unit cell was optimized at resonant frequency 5.15 GHz by using parametric analysis of CST. The CSRR unit cell consisting of three circular slit rings were etched in a square metal. The square metal was placed on square Rogers RT6002 (lossy) substrate having ε_r = 2.92 as illustrated in figure 4.10 below.

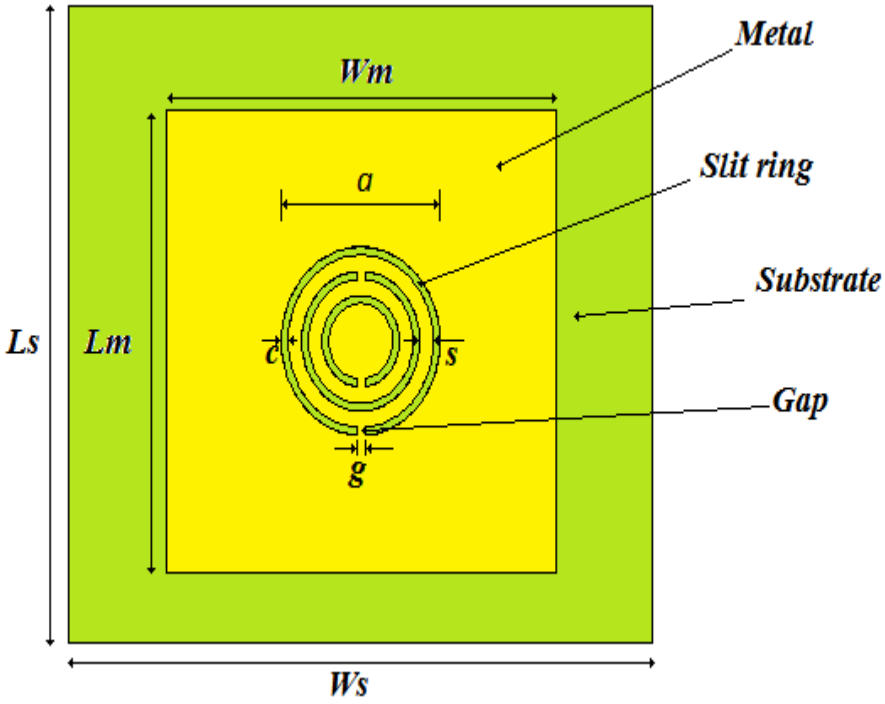

Figure 4.10: CSRR Structure

The optimized parameters of CSRR unit cells are shown in table 4.2. The main condition to design CSRR is the diameter of the outer ring 'a' and should be less than the wavelength at 5.15 GHz, ($a << \lambda$)[20] [21].

Table 4.2: Optimized Parameters of CSRR Unit Cell Structure.

Parameters of the CSRR	**Definition of the parameters**	**Values of parameters mm**
W_s	The width of substrate	26
L_s	The length of substrate	26
W_m	The width of CSRR unit cell	14.69
L_m	The length 0fCSRR unit cell	14.69
s	The width of metal rings	0.51
c	The width of slit rings	0.25
g	The width of metal gap	0.3
h	The thickness of substrate	0.762
t	The thickness of metal	0.035

TEM waveguide method was used to excite CSRR unit cell structure [22] [23]. CSRR unit cell structure embedded at the middle of a TEM waveguide (which has two waveguide ports) are used. The perfect magnetic conductor (PMC) boundary condition is applied to the y-axis, whereas, the perfect electric conductor (PEC) boundary condition is applied to the z-axis. A time-domain solver was used for the simulation. The simulation model is illustrated in figure 4.11 below.

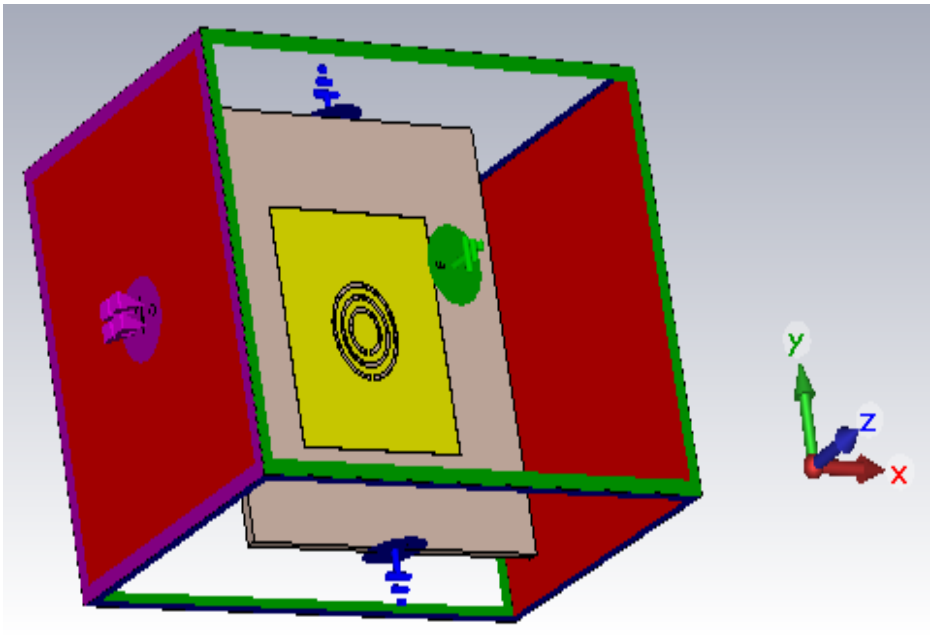

Figure 4.11: CSRR Unit Cell Structure Embedded in a TEM Waveguide

The simulation process of CSRR unit cell is done by CST. Figure 4.12 below demonstrates the S-parameter characteristics of the circular CSRR unit cell at different values of the outer ring diameter.

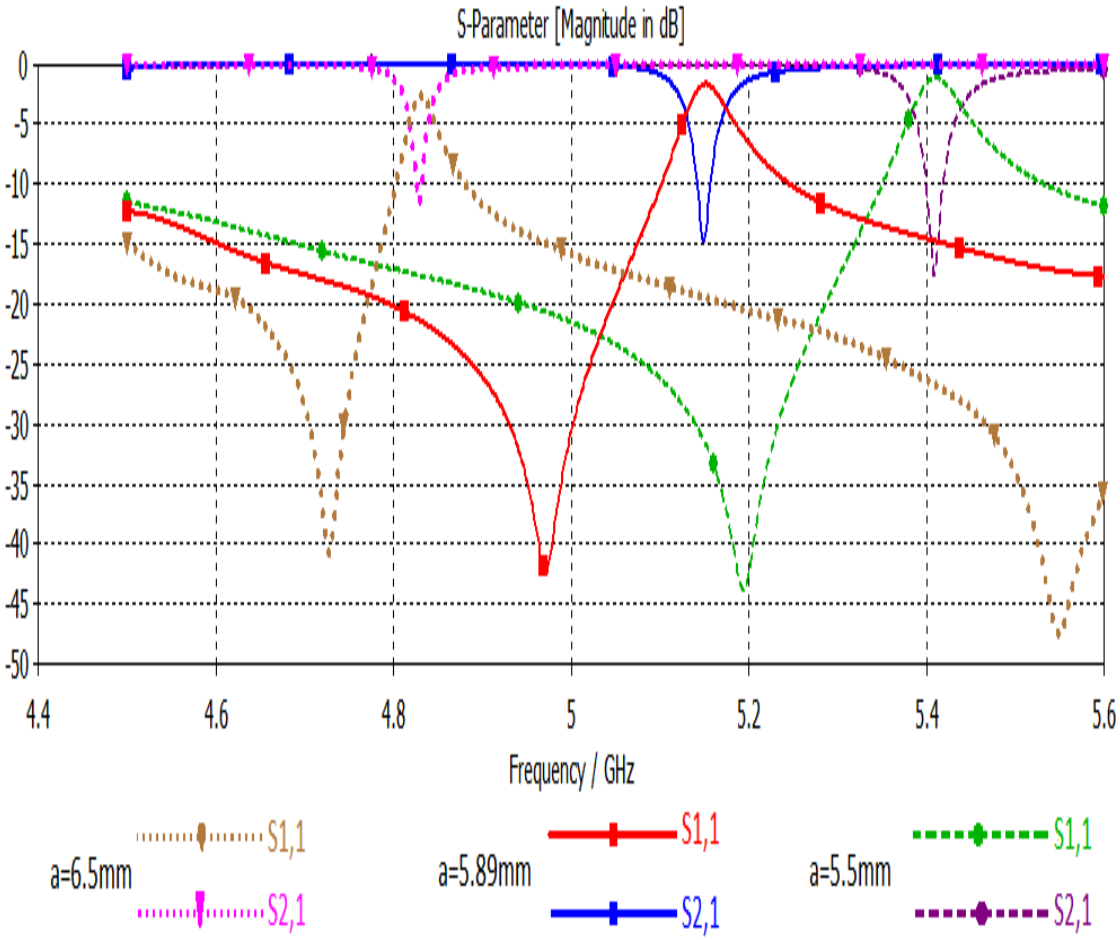

Figure 4.12: S-parameters of the Circular CSRR Unit Cell.

As illustrate in the figure 4.12, CSRR unit cell has resonant at desired frequency when a = 5.89 mm. By using NRW method, the permittivityε_r of CSRR unit cell at resonant frequency 5.15 GHz was calculated. Microsoft excel was used to plot the curve of permittivity ε_r as shown in figure 4.13.

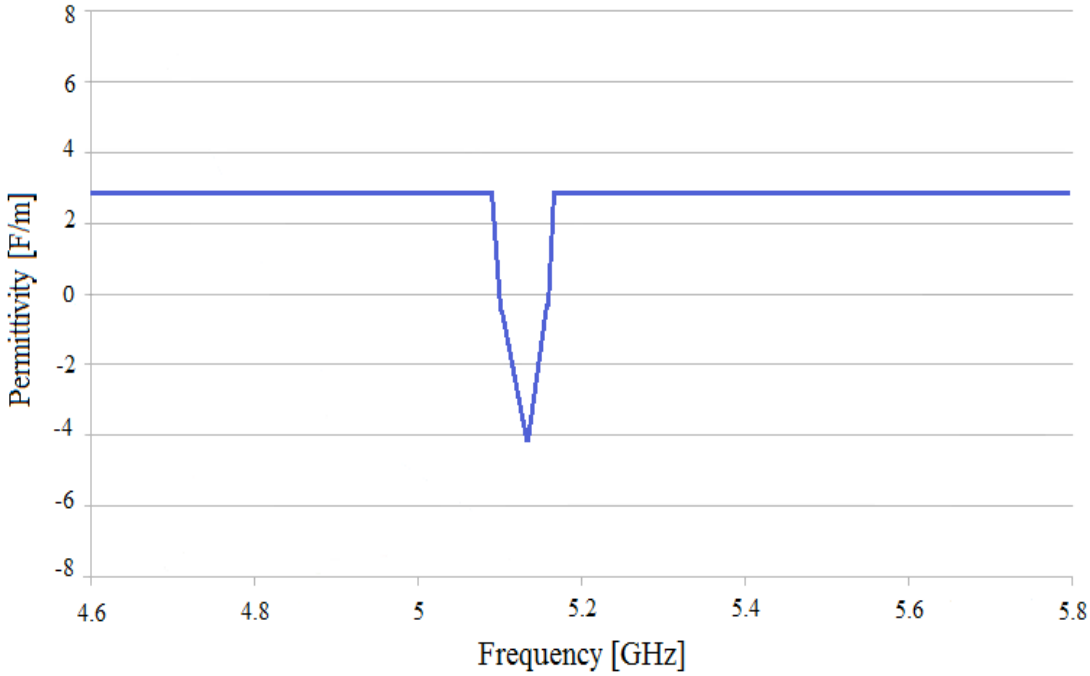

Figure 4.13: Real Values of Permittivity $\boldsymbol{\varepsilon_r}$

4.3.2 MMPA Design

The purpose of using CSRR in substrate, the resonance frequency of MMPA will shift to CSRR unit cell resonance frequency at the desired frequency [3]. The design of MMPA was optimized at resonant frequency f_r=5.15 GHz with CSRR unit cell. MMPA consists of two separate Rogers RT6002 (loss) substrates, which has permittivity ε_r=2.92, substrate thickness of h= 0.762 mm for each. CSRR unit cell is placed in between the patch and the ground. All values of the optimized parameters are shown in table 4.3.

Table 4.3: Optimized Parameters of MMPA

Parameters of the antenna	**Definition of the parameters**	**Values of parameters mm**
W_s	Substrates width	26
L_s	Substrates length	26
W_p	Patch width	7
L_p	Patch length	7
W_f	Feed line width	0.96
L_f	Feed line length	14
W_g	Inset feed width	1.96
y_o	Inset feed length	2.6
T	Thickness of the patch	0.035

4.3.3 MMPA Results

The design of MMPA is done by CST. Figure 4.14 below represents 3D structure of MMPA in CST.

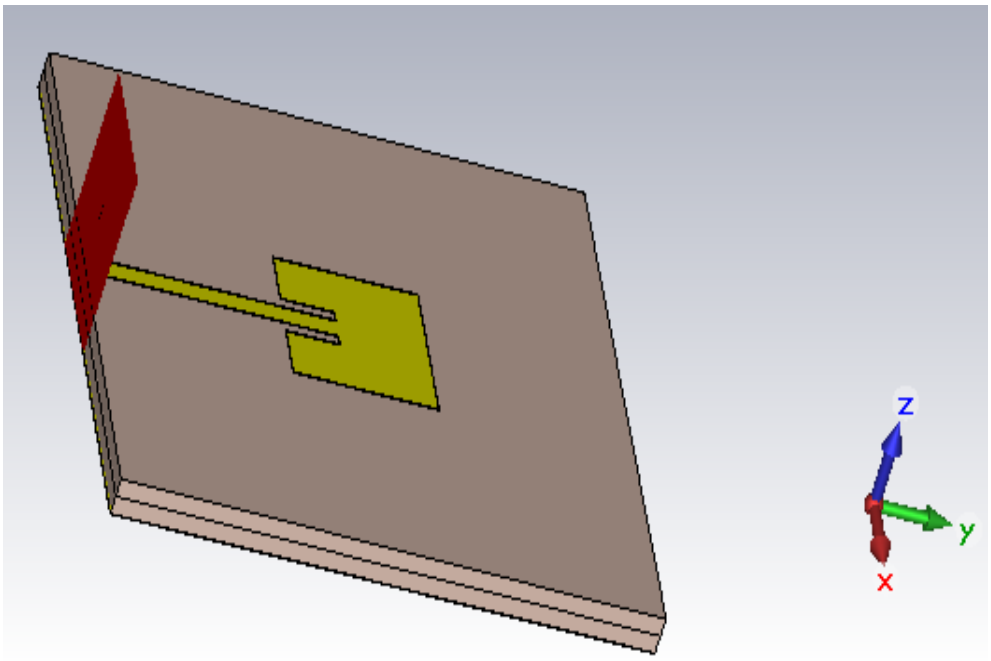

Figure 4.14: MMPA Structure in CST

For more illustration, MMPA design has been simulated at three different values of outer slit ring diameter of CSRR unit cell, whereas, the size of MMPA was fixed. Figure 4.15 shows the return loss of MMPA at different size of CSRR unit cell.

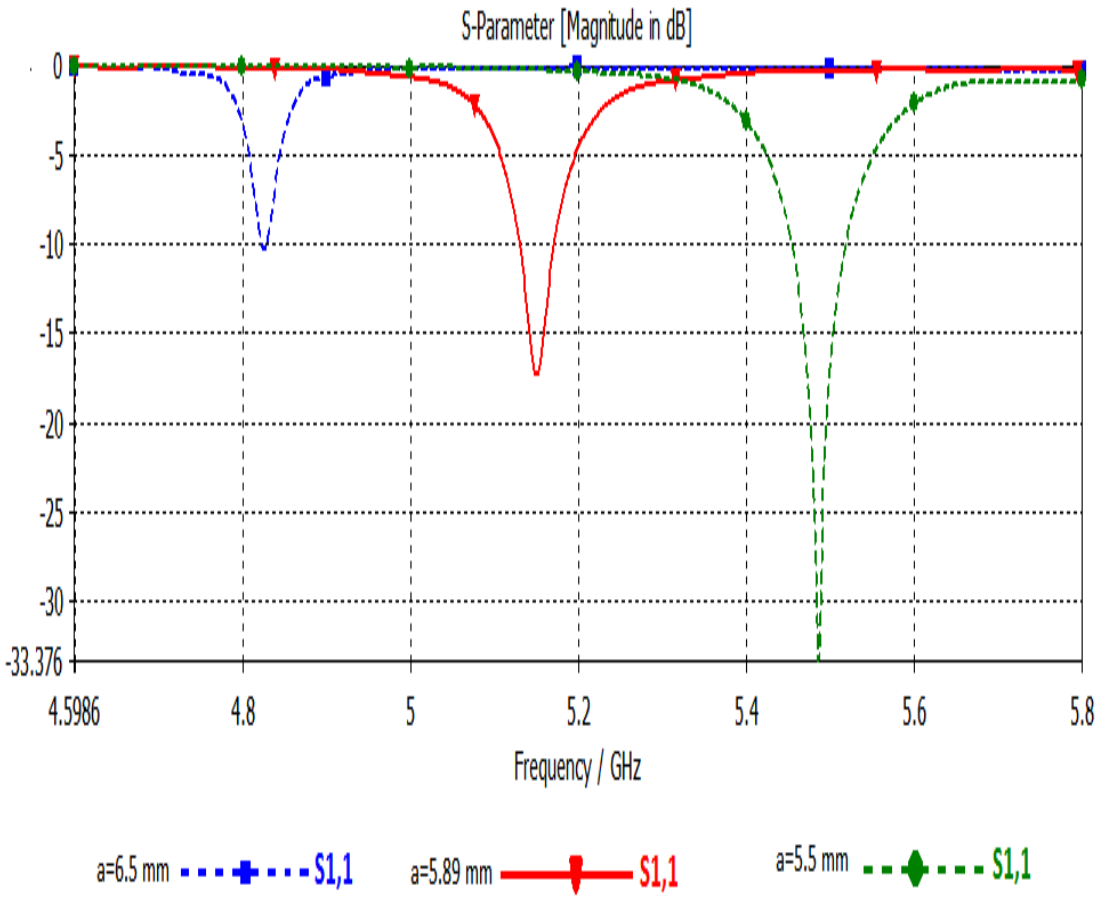

Figure 4.15: Return Loss of MMPA at Different CSRR Unit Cell Size

As represented in figure 4.15 the simulation result of MMPA were investigated at three different values of CSRR unit cell. MMPA has resonant frequency at 5.15 GHz and the return loss is -17.369 dB when the values of outer slit ring diameter of CSRR unit cell is a = 5.89 mm. The bandwidth efficiency of MMPA at -10 dB is 0.8 % by calculation as represented in figure 4.16.

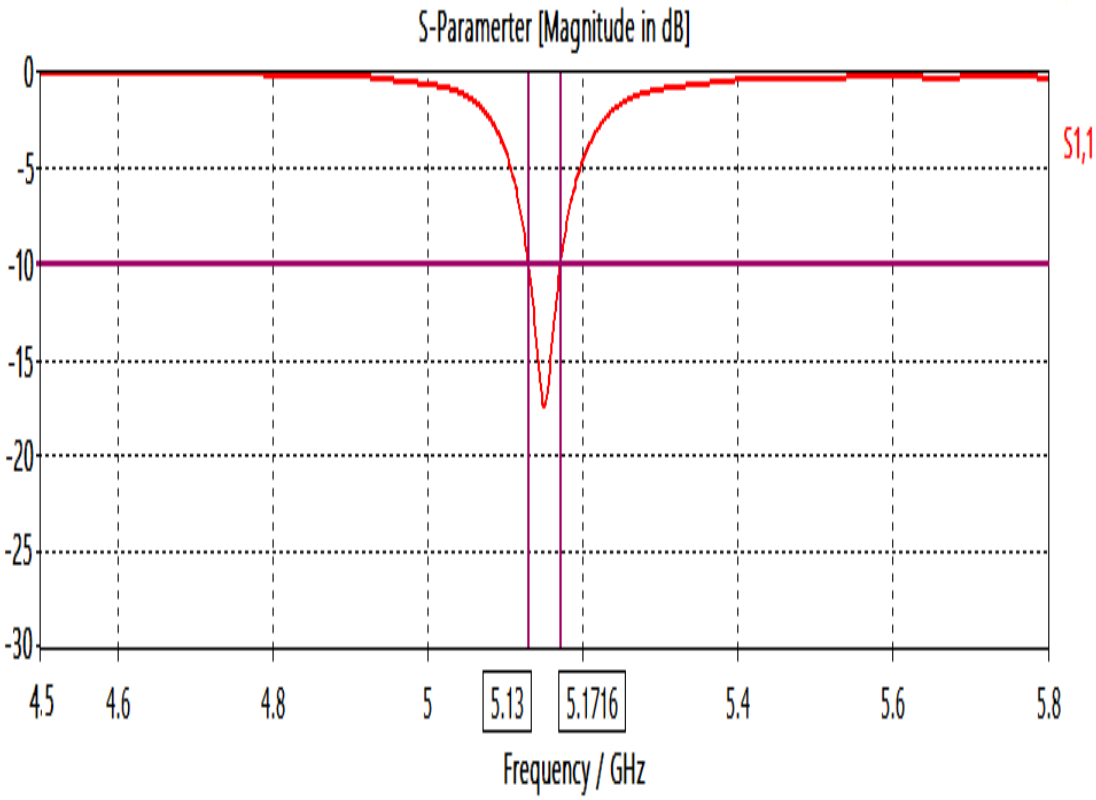

Figure 4.16: Return Loss of MMPA

The gain of MMPA is 5.76 dB as shown in figures 4.17 and 4.18 below.

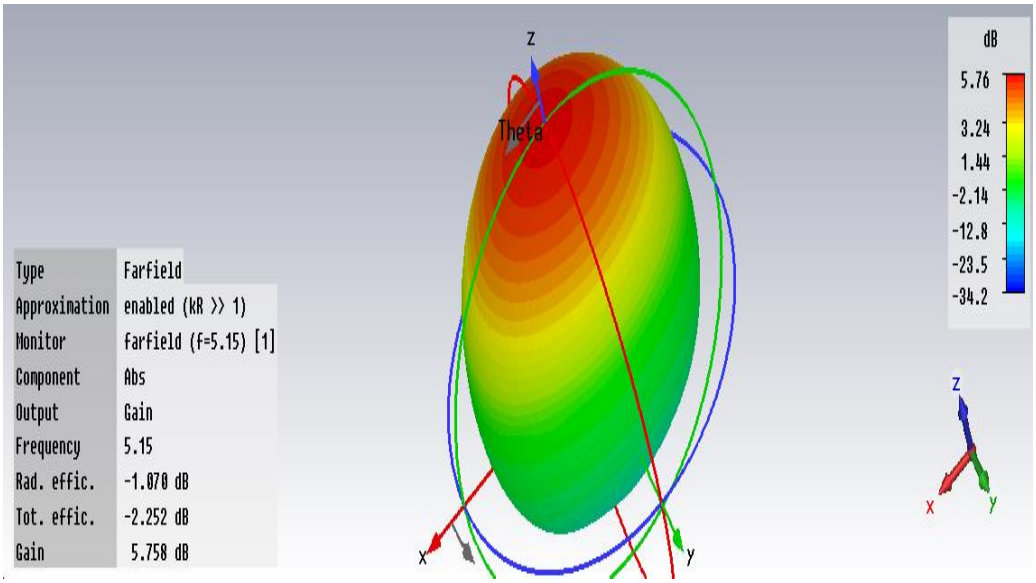

Figure 4.17: 3D Gain of MMPA in dB

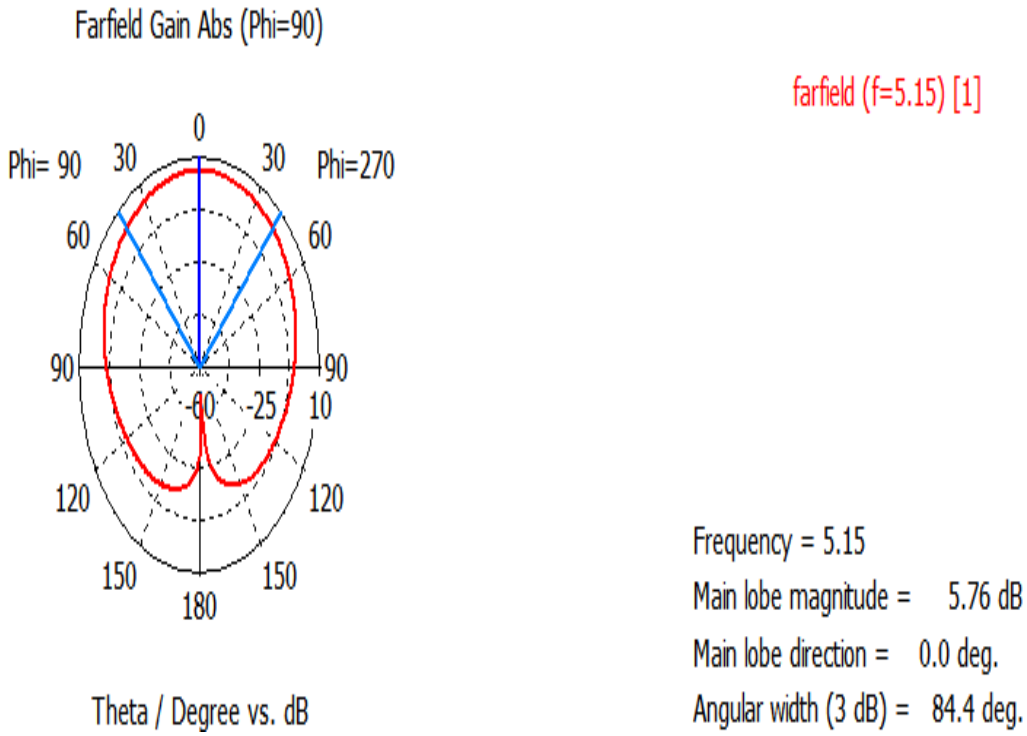

Figure 4.18: Polar Plot of Antenna Gain of MMPA

The antenna directivity of MMPA is 6.83 dBi as shown in figures 4.19 and 4.20 below.

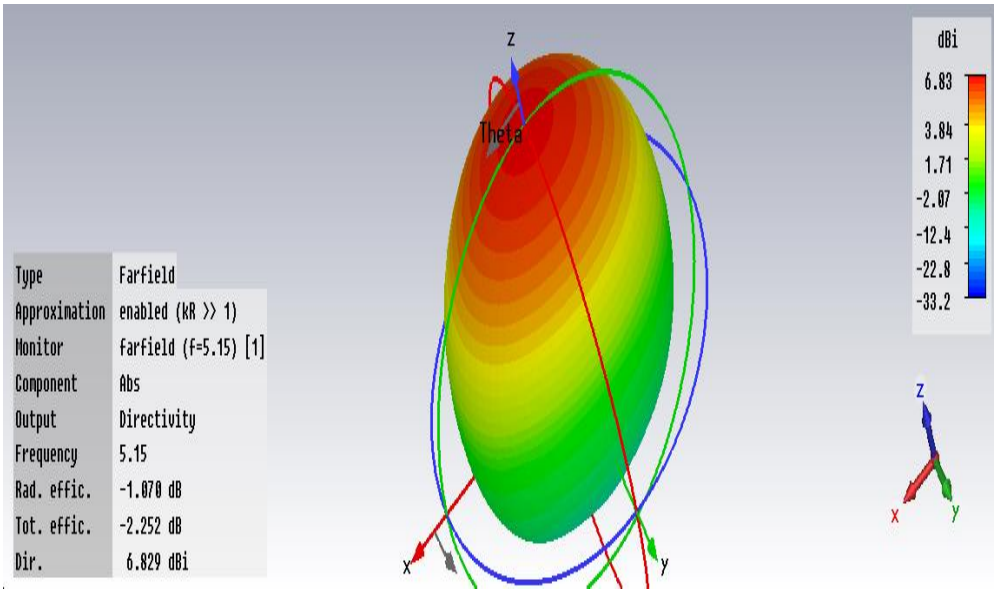

Figure 4.19: 3D Directivity of MMPA in dBi

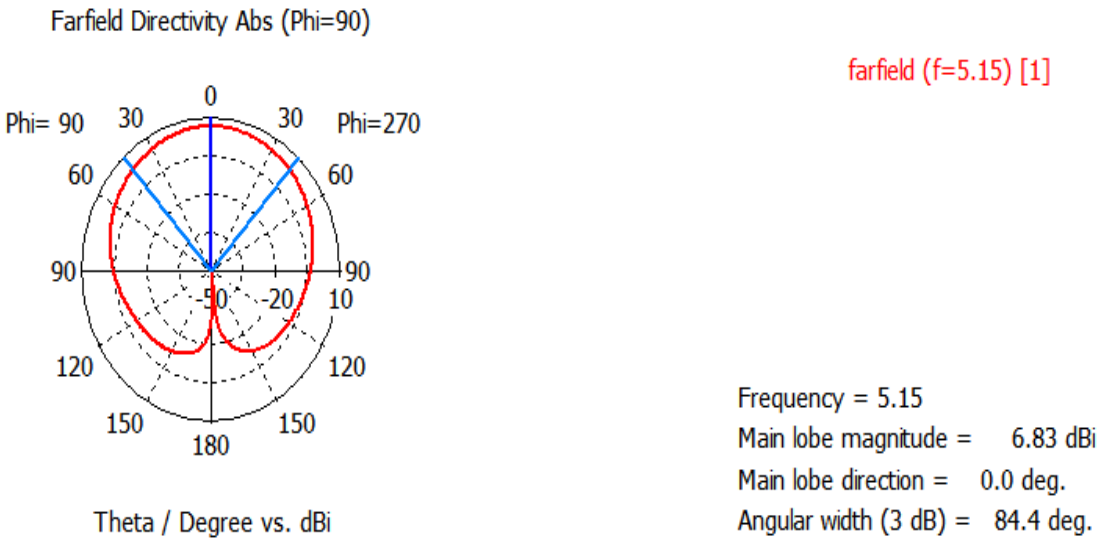

Figure 4.20: Polar Plot of Antenna Directivity of MMPA

4.4 Results Discussion

In this part, a discussion on the results of simulation of CMPA and MMPA is made. The return loss of CMPA was -25.004 dB at frequency resonator 5.15 GHz better than the return loss of MMPA which was -17.369 dB. Figure 4.21 illustrates the return loss of CMPA and MMPA.

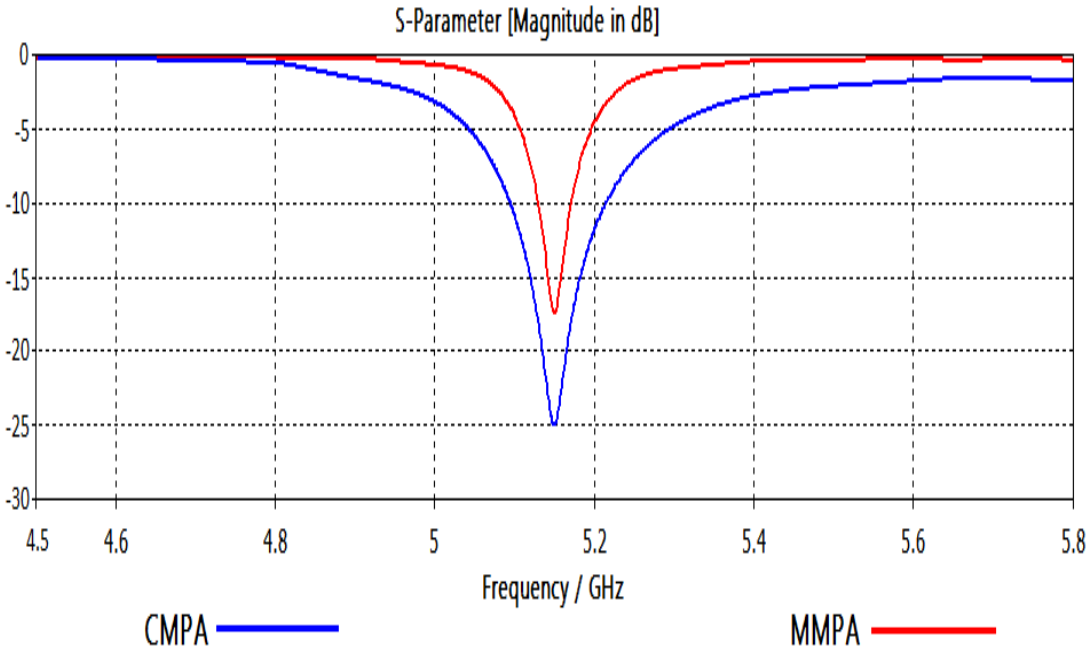

Figure 4.21: Return Loss of CMPA and MMPA

Results show that, the directivity of CMPA has slightly dropped from 7.29 dBi to 6.83 dBi in MMPA. Consequently, gain of 7.22 dB is decreased to 5.76 dB. In addition, the band width efficiency of 2.3 % is dropped to 0.8 % in MMPA and the antenna efficiency has little reduction from 98.4 % to 78.16 % in MMPA. On the other hand, the size of the patch antenna was reduced from 254.402 mm^2 to 49 mm^2 and the ratio of size reduction was reached to 80.7 % for the patch.

4.5 Antenna Design and Results of [6]

The results of this study are compared with the results of the reference paper titled "A Miniaturized Patch Antenna by Using CSRR Loading Plane" [6]. In the reference paper, there are two designs. The design of CMPA called as traditional antenna in the paper, consists of three layers, square patch, substrate and ground plane. The design of MMPA called as miniaturized antenna in the paper, consists of five layers, square patch, ground plane and CSRR plane having three square slip rings, which are placed between two substrates as shown in figure 4.21. The type of substrate which is used for both designs is Rogers RT6002 (lossy) with permittivity (ε_r= 2.92). Substrate thickness is (h=1.524 mm) for the traditional antenna, where the thickness is (h = 0.762 mm) for substrate 1 and 2. Both designs used microstrip line with quarter wave transformer impedance to feed the antenna as shown in figure 4.22 below.

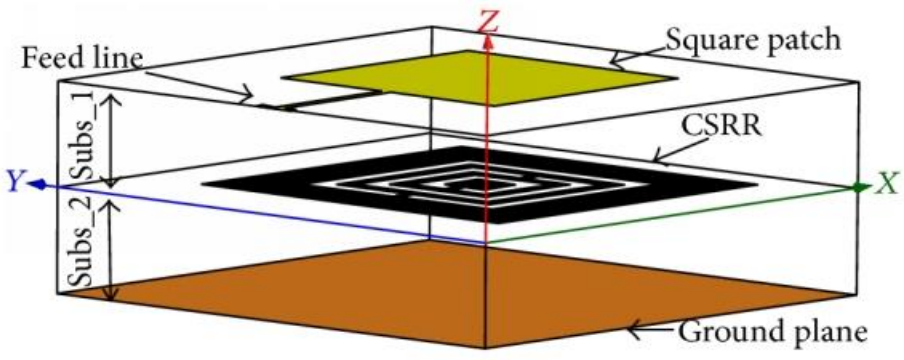

Figure 4.22: 3D Structure of Miniaturized Antenna of [6]

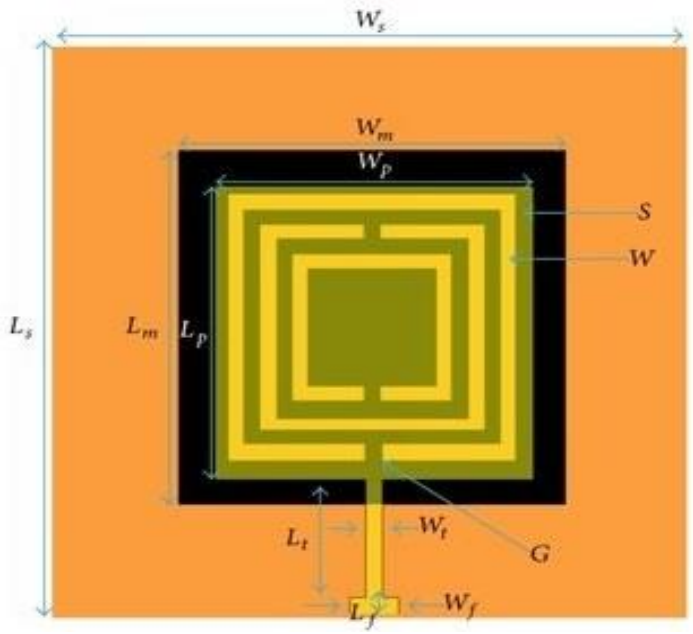

Figure 4.23: Top View of Miniaturized Antenna with Physical Parameters of [6]

The parameters of traditional and miniaturized antennas are shown in table4.4.

Table 4.4: Physical Parameters of Traditional and Miniaturized Antennas of [6]

Parameters of the antennas	**Traditional antenna (mm)**	**Miniaturized antenna (mm)**
Ws	40	28
Ls	40	28
Wp	15.95	8
Lp	15.95	8
Wf	4	4
Lf	4	1
Wt	0.7	1.2
Lt	9	14.4
Wm	-	14.4
Lm	-	14.4
S	-	0.51
G	-	0.3
W	-	0.25

The simulation results of the reference paper were done by using ANSYSHFSS software. Figure 4.24 shows the return loss of traditional and miniaturized antennas in the reference paper.

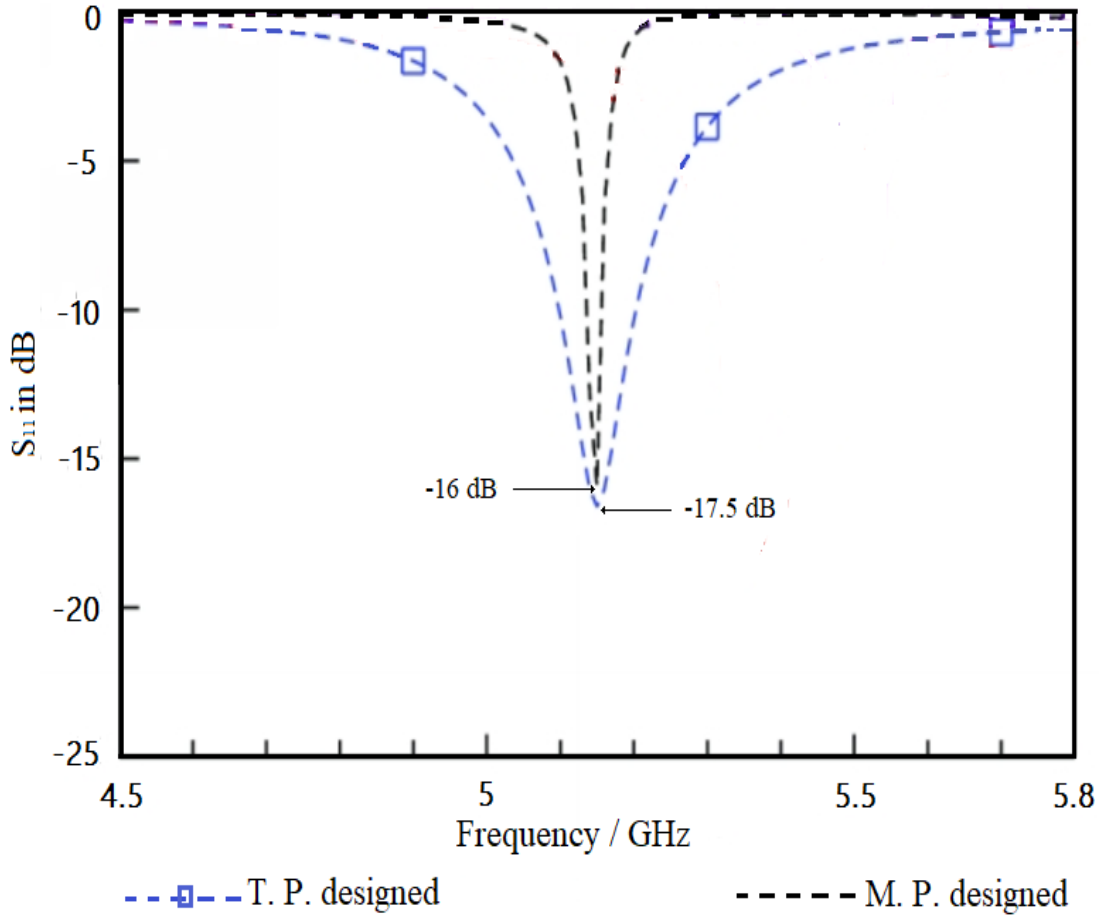

Figure 4.24: Return loss of Traditional and Miniaturized Antennas of [6]

4.6 Comparison of Results

The comparison will be between the new design and the reference paper in terms of the simulation results and designs. Table 4.5 shows the most important point of the comparison.

Table 4.5: Comparison between Results of this Study and [6]

Parameters	The thesis		Reference paper	
	CMPA	**MMPA**	**Traditional antenna**	**Miniaturized antenna**
Patch size (mm^2)	254.4	49	254.4	64
Metamaterial shape	-	Circular ring	-	Square ring
Feed technique type	Microstrip line with inset feed	Microstrip line with inset feed	Microstrip line with impedance quarter wave transform	Microstrip line with impedance quarter wave transform
Return loss (dB)	-25.004	-17.369	-17.5	-16
Gain (dB)	7.22	5.76	7.35	5.72
Directivity (dBi)	7.29	6.83	7.39	6.78
Bandwidth efficiency (%)	2.3	0.8	2	0.4
Antenna efficiency (%)	98.4	78.16	99	78.3
Reduction ratio (%)	-	80.7	-	74.8

The comparison demonstrates that patch size of MMPA is 49 mm^2 in this study is smaller than the patch size of miniaturized antenna which was 64 mm^2 in the reference paper. With reduction ratio 80.7 % the value in current study is significantly better than the reduction ratio in the reference which is 74.8 %. In addition, the gain 5.76 dB and directivity 6.83 dBi of MMPA are better than gain 5.72 dB and directivity 6.78 dBi of the miniaturized antenna in the reference paper. In total, the thesis achieves smaller size with better performance of MMPA.

Chapter 5

CONCLUSION AND FUTURE WORK

5.1 Conclusion

The important goal of this study, is to reduce the size of CMPA, which has resonant frequency 5.15 GHz by using metamaterial substrate. CSRR metamaterial unit cell was placed in the substrate to make artificial dielectric. The reduction size was achieved in MMPA, which has smaller dimensions than CMPA and both antennas have resonant frequency of 5.15 GHz.

The return loss (S_{11}) for both design was less than -10 dB at the resonant frequency. This implies that the matching impedance is achieved by using microstrip line feed with inset cut in the patches. The results of this study were successful when compared with the results of [6], reduction ratio recorded in this study was 5.9 % more than reduction ratio in documented reference paper. Overall, all the planed works and the objectives of this study were successfully carried out and considered accomplished.

5.2 Future Work

The suggestion in this study proposes for future research to seek to achieve high reduction ratio of MMPA that operate at 5.15 GHz frequency by using metamaterial structure. Future study will also will include the use of CSRR unit cell in different position (for instance, etch CSRR unit cell on ground plane or on patch) to increase reduction ratio and performance of the patch antenna.

REFERENCES

[1] V. Kambo, J. G. Saini and A. Saini, "Miniaturization of microstrip patch antenna using slots for S band", *International Journal of Engineering Science and Computing*, July. 2016.

[2] R. Porath, “Theory of miniaturized shorting-post microstrip antennas”, *IEEE Transactions on Antennas and Propagation*, Vol. 48, No. 1, January. 2000.

[3] A. G. Jahromi, F. Mohajeri, and N. Feiz, “Miniaturization of a rectangular microstrip patch antenna loaded with metamaterial”, *International Journal of Electrical, Computer, Energetic, Electronic and Communication Engineering*, 2013.

[4] C. H. Hsu, C. H. Lai, and Y. S. Chang, “A compact planar microstrip-fed feed patch antenna using high permittivity substrate”, *Electromagnetic Research Symposium Proceedings. Suzhou. China*, Septemper. 12. 2011.

[5] S. Islam and M. Latrach, "Design construction and testing of a compact size patch Antenna for RFID applications", *Microwave and Optical Technology*. Letters 55(12), pp. 2920-2925, 2013.

[6] M. Ramzan and K. Topalli, "A miniaturized patch antenna by using a CSRR loading plane", *International Journal of Antennas and Propagation*. Article ID 495629, 9 pages, 2015.

[7] Y. Huang and K. Boyle, “Antennas from theory to practice", A *Short History of Antennas*, pp. 1-5, 2008, John Wiley & Sons Ltd, The Atrium, Southern Gate. Chichester. West Sussex, PO198SQ. United Kingdom.

[8] B. D. Patel, "Microstrip patch antenna- A historical perspective of the development", *Conference on Advances in Communication and Control Systems,* 2013.

[9] A. Kaur, A. Singh and E. Sidhu, " Comparative study of square CSRR and circular CSRR structure on microstrip patch Antenna for WLAN applications”, *International Journal of Advanced Research in Electronics and Communication Engineering*, vol 3, Issue. 8, August, 2014.

[10] B. Choudlhury, “Metamaterial inspired electromagnetic applications role of intelligent systems”, *Introduction*, pp 23- 25, 2017, Springer Nature Singapore Pte Ltd, Bangalore. Karnataka, India.

[11] V. G. Veselago, “The electrodynamics of substances with simultaneously negative values of ε and μ”, *Soviet Physics Uspekhi*, vol. 10, no. 4, Jan-Feb.1968.

[12] Dr. Smith, W.J. Padilla, D.C. Vier Nemat Naseer and S. Schultz, “Composite medium with simultaneously negative permeability and permittivity”, *phys. Rev. letters*, vol. 84, pp 4184-87, 2000.

[13] Preetkaur, Dr. S.K. Aggarwal and Dr. Asok, " A survey of techniques used for performance enhancement of patch antenna using metamaterials", *IOSR Journal of Electronics and Communication Engineering*, vol. 10, PP 98-109, December. 2015.

[14] J. B. Pendry, A. J. Holden, D. J. Robbins and W. J. Stewart, "Magnetism from conductors, and enhanced non-linear phenomena", *IEEE Trans. Microwave Theory Tech*, vol. 47, pp.2075-84, 1999.

[15] J. D. Baena, J. Bonache, F. Martin, R. Marques, F. Falcone, T. Lopetegi, M. A. G. Laso, J. Garcia, G. Ignacio and M. F. Portillo, "Equivalent circuit models for split ring resonators and complementary split ring resonators coupled to planar transmission lines", *IEEE Transactions on Microwave Theory and Techniques*, vol. 53, no. 4, 2005.

[16] F. Falcone, T. Lopetegi, J. D. Baena, R. Marqus, F. Martn, and M. Sorolla, "Effective negative stop-band microstrip lines based on complementary split ring resonators", *IEEE Microwave and Wireless Component Letters*, vol. 14, pp. 280-282, 2004.

[17] L. Rohde and H. Schwarz, " Measurement of dielectric material properties", *Nicholson-Ross-Weir Conversion Process. Application Centre Asia/Pacific*, 2006.

[18] N. Ripin, W. M. A. W. Saidy, A. A. Sulaiman, N. E. A. Rashid and M. F. Huss, " Miniaturization of microstrip patch antenna through metamaterial approach", *IEEE Student Conference on Research and Development*, 2013.

[19] R. A. H. Mahdi, Dr. Saleem and M. R. Taha, "Miniaturization of rectangular microstrip patch antenna using topology optimized metamaterial", *IEICE Electronics Express*, September.13. 2017.

[20] H.M. Elkamchouchi, A.A. Sheshtawy and A.I. Almahallawy, "Study and Investigation of complementary split ring resonators (CSRR) metamaterials and its application in microstrip antenna design", *International Journal of Applied Engineering Research*, ISSN 0973-4562, vol. 11, no. 4, pp 2791-2795, 2016.

[21] G. Lubkowski, B. Bandlow, R. Schuhmann and T. Weiland, " Effective modelling of double negative metamaterial macrostructures", *IEEE Transactions on Microwave Theory and Techniques*, vol. 57, no. 5, May. 2009.

[22] S. Hrabar and J. Bartolic, "Backward wave propagation in waveguide filled with negative permeability metamaterial*", Antennas and Propagation Society International Symposium*, vol. 1, pp 110 – 113, 2003.

[23] S. Hrabar, G. Jankovic, B. Zivkovic and Z. Sipus, "Numerical and experimental investigation of field distribution in waveguide filled with anisotropic single negative metamaterial", *Applied Electromagnetic and Communications*, pp 1- 4, 2005.